UNIVERSITATEA TITU MAIORESCU BUCUREȘTI

IOSUD

Field MEDICINE

DOCTORAL THESIS

STUDIES ON THE ANTIMICROBIAL AND ANTIOXIDANT EFFECT OF SOME NATURAL BIOACTIVE COMPOUNDS; REALIZATION OF COMPLEXES BASED ON GOLD AND SILVER NANOPARTICLES BY GREEN SYNTHESIS WITH BIOACTIVE COMPOUNDS FROM PLANT EXTRACTS

Summary

Scientific Supervisor

Prof. univ. dr. habil. CRISTIANA TĂNASE

Doctorand

Daniel CORD

BUCHAREST

2025

CONTAINED

List of abbreviations

NF-κB =factorul nuclear-kappa
ADN= acid dezoxiribonucleic
REL= virusuri a reticuloendoteliozei
UV= ultraviolet rays
MMP= matrix metaloproteaze
VEGF= endothelial vascular growth factor
COX-2 = cyclooxygen-2
IkBα= Inhibitor al factorului nuclear kappa B, izoforma alpha
JAK=janus kinază
CAPE= phenethyl ester of caffeic acid
TNF= tumor necrosis factor
TNFα= casectin
TNF-β= limfotoxin
IL-1= interleukin-1
IL-8= interleukin-8
LOX-2 = lipoxygenaze-2
uPA= urokinase plasminogen activator
JNK= kinaza N-terminală c-Jun
MEK= Mitogen-activated extracellular protein kinase kinase
Cdk-4= cyclin-dependent kinase 4
Cdk-6= cyclin-dependent kinase 6
Cdk-7= cyclin-dependent kinase 7
Cdc2= cell division iclu 2
NO=nitrogen oxide
ROS = reactive oxygen species
RNS= reactive nitrogen species
HIF= hypoxia-inducible factor
PAMP= molecular patterns associated with pathogens
iNOS= inducible nitrogen oxide synthase
Cdk= Cyclin kinase dependent
EGF= epidermal growth factor
PDGF = platelet-derived growth factor
fibroblastic growth factors (FGF),
Epo=erythropoietin
IGF=insulin-like growth factor
IL=interleukin
AP-1=proteina activator 1
AuNPs= gold nanoparticles
AgNps=nanoparticule argint
SAgNPs-WT = silver nanoparticles obtained from Salix alba
AuNPsEETOH = gold nanoparticles obtained from ethanoic pelinite extract
AuNPSEaqSW=gold nanoparticles obtained by aqueous pelinite extract
EETOH-SW =extract etanolic de peliniță
Eaq-SW = extract apos peliniță
IMTB=imatinib
SNTB= sunitinib

INTRODUCTION

In recent decades, interest in the use of natural bioactive compounds in modern therapies has increased significantly due to outstanding biological properties, including antiproliferative, antimicrobial, antioxidant and antiinflationary activity. Herbs are an important source of secondary metabolites with therapeutic potential, and numerous studies have demonstrated their effectiveness in the prevention and treatment of severe conditions, including cancer and infectious diseases.

In the context of increasing microbial resistance to antibiotics and conventional limitations against conceration, the development of new therapeutic approaches based on natural compounds is becoming a necessity. The mechanisms of the immune response to microbial infections and the strategies for intensifying it are essential aspects in the discovery of effective antimicrobial agents. In this sense, plants such as *Artemisia annua, Silybum marianum, Chelidonium majus, Taraxacum officinale and Salix alba* have been intensively studied for their phytochemical composition and their ability to modulate critical biological processes.

Nanotechnologies offer a new dimension in harnessing the therapeutic potential of these natural compounds. Nanoparticles, especially gold and silver, have demonstrated exceptional antimicrobial and antitumor properties, and their synthesis by "green" methods using plant extracts reduces toxicity and negative environmental impact. The synergism between biosynthesized nanoparticles and antitumor therapies can lead to the creation of advanced drug delivery systems that allow selective and effective targeting of tumor cells.

The experimental part of this paper contains *in vitro* studies of the antimicrobial and tumor activity of plant extracts and biosynthesized nanoparticles, highlighting their impact on tumor lines. The physicochemical properties of nanoparticles and their antibiofilm effects against antibiotic-resistant bacteria are also evaluated.

Finally, this thesis aims to contribute to the development of innovative pharmaceutical products based on the combination of bioactive plant compounds and nanotechnologies, aiming to improve current therapies for microbial infections and oncological diseases. Future studies will be directed towards optimizing formulations, evaluating their safety and patenting the developed compositions, opening up new natural perspectives in modern medicine.

SPECIAL PART

4. STUDIES ON THE ANTIMICROBIAL AND ANTIOXIDANT EFFECT OF EXTRACTS FROM *SILYBUM MARIANUM*, *ARTEMISIA ANNUA*, *TARAXACUM OFFICINALE* AND *CHELIDONIUM MAJUS*

4.1 INTRODUCTION

The purpose of this chapter is to study the antimicrobial and antioxidant activity of some extracts of *Taraxacum officinale* (tincture), *Chelidonium majus* (tincture), *Silybum marianum* (tincture) and *Artemisia annua* (alcoholic extracts). In order to achieve this goal, the following objectives were proposed:

A. Antioxidant capacity

1. Determination of total polyphenol content
2. Determination of total flavonoid content
3. Determination of antioxidant action

B. Antimicrobial capacity

1. Qualitative assessment of antimicrobial activity
2. Quantitative determination of antimicrobial activity
3. In *vitro investigation* of anti-biofilm properties

A new direction of research is represented by the exploitation of the antimicrobial properties of large varieties of plants, which represent a reservoir that provides numerous compounds useful in the fight against multi-resistant microorganisms [206].

Taraxacum officinale, commonly known as dandelion, is a medicinal plant that has been used for centuries for its benefits in the treatment of conditions such as gallbladder, to improve liver function, lower blood pressure and blood cholesterol levels, or for its diuretic effect. In addition, studies in the literature have shown that the infusion made from this plant has beneficial effects on the renal calicles [207].

Chelidonium majus, rostopasca, is one of the oldest and most widely used plants in traditional medicine. Its benefits are multiple, being often used in the treatment of eczema and warts caused by Human Papilloma Virus (HPV) infection, liver and gastric diseases, as well as having anti-inflammatory and analgesic effects [208-210].

The therapeutic properties of extracts obtained from *Silybum marianum* (milk thistle) have been known for centuries due to its frequent use in traditional medicine to treat various liver conditions, such as jaundice. Currently, numerous clinical and experimental studies have

demonstrated that *S. marianum* is a hepatoprotective agent, with anti-inflammatory and antioxidant functions due to the presence of silymarin, being also used in the treatment of poisoning with *Amanita muscaria* [211-212].

Artemisia annua is one of the most famous medicinal plants used today, its main property being represented by its antimalarial activity, a discovery that was honored with the Nobel Prize in Medicine in 2015.

Moreover, specialized studies have demonstrated its effectiveness in the treatment of multiple diseases, such as asthma, rheumatoid arthritis, tuberculosis, herpes, or hepatitis B and C viruses. In addition, other important pharmacological functions are represented by the anti-cancer and anti-tumor properties [213-214].

4.2. MATERIAL AND METHOD

A. ANTIOXIDANT CAPACITY

4.2.1 DETERMINATION OF TOTAL POLYPHENOL CONTENT

The determination of the total polyphenol content was performed using the Singleton spectrophotometric method, based on the measurement of the absorbent of the solution obtained by the reaction between the polyphenols and the Folin-Ciocalteu reagent, at a wavelength of **765 nm**. Gallic acid was used as a standard for quantification.

For this analysis, **ethanolic extracts (50%)** were prepared from the dry plant material, in a concentration of **1%.** The samples analyzed included: *Chelidonium majus, Artemisia annua, Taraxacum officinale, Silybium marianum, Salix alba*

The plant material was subjected to reflux extraction for **30 minutes** on a water bath, followed by filtering and filling the volume to the mark in a quoted flask. For analysis, **1 mL of ethanol extract** was mixed with **5 mL of Folin-Ciocalteu reagent** (diluted **10 times** with distilled water) and **4 mL of 7.5% sodium carbonate solution**.

The reproducibility of the method was verified by the linearity of the regression curve and the value of the coefficient of determination r2 (0.999439), calculated using the Analyst software of the spectrophotometer. All regents were analytical grade and solvents were HPLC grade.

4.2.2 DETERMINATION OF ANTIOXIDANT ACTION

The method for determining the antioxidant action of plant extracts is based on the capture of the radical 2,2-diphenyl-1-picrylhydrazil (DPPH). For this, ethanolic extracts (50%) in a concentration of 1% of dried vegetable products were obtained by reflux on a water bath for 30 minutes, filtration and filling in a quoted flask.

B. ANTIMICROBIAL CAPACITY

In this study, a number of **6 extracts were analyzed**: tincture of *Taraxacum officinale* (dandelion); tincture of *Chelidonium majus* (rosehip); tincture of *Silybum marianum* (milk thistle); alcoholic extract from mature seed plant *Artemisia annua* (pelinita); alcoholic extract from flowering plant *Artemisia annua* (peliniță); alcoholic extract from the plant before flowering *Artemisia annua* (pelinite).

Reference microorganisms were tested, two Gram-negative bacterial strains**:** *Escherichia coli* ATCC 25922 and *Pseudomonas aeruginosa* ATCC 27853, two Gram-positive strains: *Staphylococcus aureus* ATCC 25923 and *Enterococcus faecalis* ATCC 29212 and one fungal strain: *Candida albicans* ATCC 10231.

Culture media and reagents

- Mediu PCA (Plate Count Agar)

  Casein Enzyme Digest..... 5.0g
  Extract de drojdie..... 2,5g
  Dextrose (glucose)..... 1.0g
  Agar..... 15.0g
  pH 7.0±0.2 to 25ºC

- Mediu Tryptic Soy Broth (TSB); Bulion de soia triptic

  Casein Peptone..... 17.0g
  Soy peptone..... 3.0g
  Sodium chloride..... 5.0g
  Phosphate dipotasic.....
  2.5g
  Dextrose (glucose)..... 2.5g
  pH 7.3±0.2 to 25ºC

- Sterile physiological water (AFS)

  NaCl..... 8.5g
  Distilled water..... 1000mL

- Cristal violet 1%

  Cristal violet..... 1g
  Distilled water..... 100 mL

- Acetic acid 33%

  Acetic acid..... 33 mL
  Distilled water..... 100 mL

4.2.3 QUALITATIVE ASSESSMENT OF ANTIMICROBIAL ACTIVITY

The qualitative evaluation of the plant extracts was carried out by the drop method, on solid medium with agar. ***Principle of the method****:* On the surface of a PCA medium, inoculated with a standardized microbial suspension obtained from the strain to be tested by the cloth seeding technique, a volume of 5µl of each plant extract was deposited in the droplet, at equal distances. Sensitivity to a particular plant extract can be observed by inhibiting microbial growth around the deposited droplet. **Interpretation of the results**: the antimicrobial activity of the extracts was determined by evaluating the formation of an inhibition halo around the deposited extract droplet, and measuring its diameter using a ruler.

4.2.4 QUANTITATIVE ASSESSMENT OF ANTIMICROBIAL ACTIVITY

The quantitative evaluation of the antimicrobial activity of the plant extracts was performed by the method of microdilutions in liquid medium. ***Method principle*****:** In 96-well ELISA microplates in which liquid culture medium is distributed, 1/100 diluted microbial suspensions with an initial density of 0.5 McFarland of the tested strains are inoculated in a gradient of concentrations of plant extracts. The values of the minimum inhibitory concentration (MIC) and the minimum bactericidal concentration (BAC) are determined by drip seeding on agar medium of the first 8 wells corresponding to the concentrations of 50%-0.39% of each plant extract. **Interpretation of results**: the antimicrobial activity of the extracts was determined by evaluating the development of microbial cultures on the agar medium. The CMI value represents the concentration at which the plant extract inhibits the growth and multiplication of microorganisms, having a bacteriostatic effect, and the CMB value represents the concentration at which the plant extract has a lethal action on microorganisms, having a bactericidal effect.

4.2.5 IN *VITRO ASSESSMENT* OF ANTIBIOTIC ACTIVITY

The evaluation of the antibiofilm activity of the plant extracts was tested by the 1% purple crystal microtiter method. ***Method principle****:* Following incubation of sterile ELISA microplates with 96 wells with liquid culture medium in which microbial suspensions are inoculated in a gradient of concentrations of the tested plant extracts, the in vitro antibiofilm activity of different concentrations of tinctures and alcoholic extracts is analyzed based on the values of absorption of the 1% purple crystal dye at 492 nm. **Interpretation of the results:** the antibiofilm activity of the plant extracts could be evaluated by determining the absorbance value following the spectrophotometric reading at 492 nm. The concentration of plant extracts necessary to inhibit the development of biofilms corresponds to the last well at the level at which the absorbance value is less than half of the absorbance value of the positive control corresponding to the same plant extract.

4.3. RESULTS AND DISCUSSIONS

A. EVALUATION OF ANTIOXIDANT CAPACITY

4.3.1 ASSESSMENT OF TOTAL POLYPHENOL CONTENT

The amount of polyphenols found in the studied extracts is shown in the table below:

Table I Amount of polyphenols in extracts

Plant name	Total polyphenols (mg GAE/g PV uscat)
Chelidonium majus	13,41
Artemisia annua	16,82
Taraxacum officinale	31,56
Silybium marianum	15,70
Salix alba	33,37

Of the five species analyzed, ***Salix alba*** **(33.37 mg GAE/g)** has the highest concentration of polyphenols, closely followed by ***Taraxacum officinale*** **(31.56 mg GAE/g).** These high levels suggest that these plants may have strong antioxidant and anti-inflammatory properties, making them valuable in herbal medicine, especially for treating inflammatory conditions.

On the other hand, ***Chelidonium majus*** **(13.41 mg GAE/g)** has the lowest polyphenol content, which may indicate a lower antioxidant potential compared to the other species. These results obviously do not imply a lower therapeutic efficacy, as other bioactive compounds, such as alkaloids, could contribute to its pharmacological properties.

Artemisia annua **(16.82 mg GAE/g)** and ***Silybium marianum*** **(15.70 mg GAE/g)** fall within an intermediate range, suggesting a moderate polyphenol content.

The results indicate a significant variability in the polyphenol content between the plants studied, which may influence their medicinal properties. While the concentration of polyphenols is an important factor in determining the antioxidant potential of these plants, their therapeutic value is also influenced by other bioactive compounds.

4.3.2 EVALUATION OF ANTIOXIDANT ACTION

Evaluation of the free radical scavenging capacity among selected medicinal plants reveals significant variation, suggesting differences in their antioxidant potential.

The highest free radical absorption capacity was observed in ***Artemisia annua*** **(65.44%),** followed closely by ***Taraxacum officinale*** **(59.34%).**

Table II Antioxidant action of extracts

Plant name	Ability to capture free radicals
Chelidonium Majus	27,13 %
Artemisia Annua	65,44 %
Taraxacum Officinale	59,34 %
Silybium Marianum	21,30 %
Salix Alba	40,54 %

These results indicate that these species possess a powerful antioxidant potential, due to their rich content of polyphenols, flavonoids and other bioactive compounds that contribute to their radical annihilation activity. On the other hand, ***Silybium marianum*** **(21.30%)** showed the lowest antioxidant capacity among the plants tested, followed by ***Chelidonium majus*** **(27.13%)**.

Despite their lower antioxidant capacity in this test, these plants are known for other pharmacological properties. For example, *Silybium marianum* is well known for its hepatoprotective effects, mainly attributed to silymarin, a complex of flavonolignans with antioxidant and anti-inflammatory properties.

White willow **(40.54%)** demonstrated moderate antioxidant capacity, which could be associated with its well-documented presence of phenolic glycosides, flavonoids, and tannins. The results indicate a significant variability in the activity of free radical absorption among the plant species analyzed.

While polyphenol content appears to play a role in antioxidant potential, other factors such as **the chemical structure of polyphenols, the presence of other bioactive compounds, and their interactions** may influence the observed results. Further investigations, including identification of specific compounds and *in vivo* studies, could provide deeper insight into the antioxidant mechanisms of these herbs.

The extracts of the researched plants have an important antioxidant action, due to their high content of polyphenols, which gives them a great potential for use and valorization in therapeutics.

B. ASSESSMENT OF ANTIMICROBIAL CAPACITY

4.3.4 RESULTS OF THE QUALITATIVE ASSESSMENT OF ANTIMICROBIAL ACTIVITY

This study aimed to investigate the antimicrobial properties of some plant extracts of *Taraxacum officinale* (tincture), *Chelidonium majus* (tincture), *Silybum marianum* (tincture) and *Artemisia annua* (alcoholic extracts).

In the present study, the qualitative evaluation of the antimicrobial activity of the plant extract of *T. officinale* determined an inhibition of microbial growth against the strains *E. faecalis*

ATCC 29212, *P. aeruginosa* ATCC 27853 and *C. albicans* ATCC 10231, showing inhibition halo values of 9 mm, 8 mm with weak microbial growth within the microbial inhibition zone and 8 mm with the presence of a number of of colonies inside the halo of inhibition. A resistance to the action of the plant extract was recorded in the strains of *S. aureus* ATCC 25923 and *E. coli* ATCC 25922, the presence of *T. officinale* tincture not inhibiting their microbial growth.

Chelidonium majus is a medicinal plant belonging to the *Papaveraceae family* that is found in the spontaneous flora of Europe, Asia, North America, as well as in certain regions of Africa. At the level of the composition of the extracts obtained from this plant there are quaternary alkaloids (chelerythrin, sanguinarine), tertiary alkaloids (chelidonine), proptopin, coptizin, berberine, acids such as malic, citric and hydrobenzoic acid, polyphenolic compounds, but also derivatives of hydroxycinnamic acid [218,219].

The microbial growth of the fungal strain was inhibited in the presence of the plant extract from *C. majus*, resulting in an inhibition zone value of 7 mm. The same diameter of the growth inhibition zone was recorded in the case of the *E. coli* strain ATCC 25922, and a value of 11 mm was observed in the Gram-positive strain *E. faecalis* ATCC 29212 (Table VI). This extract showed no antimicrobial activity against *S. aureus* ATCC 25923 and *P. aeruginosa* ATCC 27853.

Silybum marianum is an annual or biannual plant of the *Asteraceae* family , which is currently one of the most cultivated medicinal plants in Europe. Silybin exhibits potent antioxidant properties, modulating numerous cell signaling pathways that determine the reduction of proinflammatory mediators, and recent studies have shown the ability of this flavonolignan to inhibit serin proteases involved in blood clotting [220-222].

The study of the qualitative determination of the antimicrobial activity of the tincture of *S. marianum* on the reference strains reveals that both on the Gram-negative strains, *E. coli* ATCC 25922 and *P. aeruginosa* ATCC 27853, and on the fungal strain, *C. albicans* ATCC 10231, the plant extract did not show antimicrobial activity (Table VI). However, microbial growth inhibition could be observed in the case of the Gram-positive strains *S. aureus* ATCC 25923 and *E. faecalis* ATCC 29212, with growth inhibition zone values of 9 mm and 8 mm respectively.

Artemisia annua is an annual plant native to the Asian continent that is currently found in Europe, Australia and the United States of America. The antimicrobial, anti-inflammatory and antiparasitic properties are determined by the presence, in varying concentrations at the level of each specimen due to their cultivation and location, of secondary metabolites: flavonoid, monoterpenoid, sesquiterpenoid compounds, coumarins and aliphatic and lipid compounds [223-225].

The qualitative evaluation of the antimicrobial activity of plant extracts from *A. annua* was carried out using alcoholic extracts made from plants in 3 different stages of development: before flowering, during flowering and in the mature stage, with seeds.

A constant 10 mm microbial growth inhibition halo diameter was observed in all extracts of both *E. faecalis* ATCC 29212 and *P. aeruginosa* ATCC 27853. Similarly, the 3 alcoholic extracts inhibited the growth of *the C. albicans* ATCC 10231 strain, resulting in a growth inhibition zone value of 11 mm (Table VI).

Alcohol extracts from the plant before flowering, during flowering and with seeds showed antimicrobial activity against the Gram-negative strain *E. coli* ATCC 25922, showing inhibition zone values of 11 mm, 10 mm and 9 mm respectively (Figure 6). Antibacterial activity of the extracts was not observed in the case of *the S. aureus* strain ATCC 25923.

The analysis of the results obtained from the antimicrobial activity testing showed that the growth of the *S. aureus* strain ATCC 25923 is not inhibited by most plant extracts, a growth inhibition can only be recorded in the presence of the *S. marianum* tincture, while the E. *faecalis* strain ATCC 29212 was inhibited by all plant extracts.

S. marianum *tincture* did not show antimicrobial activity on Gram-negative and fungal strains, but it did inhibit the growth of Gram-positive strains. The alcoholic extracts of *A. anuua* used in this study exhibited the highest antimicrobial activity, resulting in an inhibitory effect on all microbial strains except *S. aureus strain* ATCC 25923 (Figure 7).

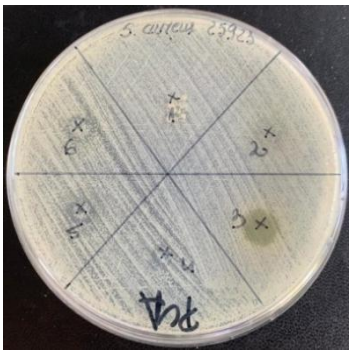

1st verse

1b front

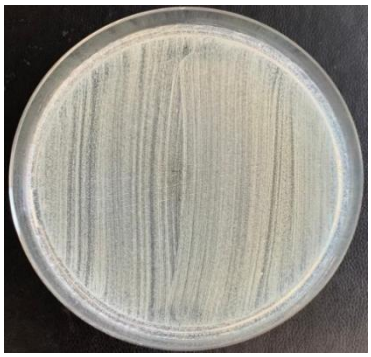

1c

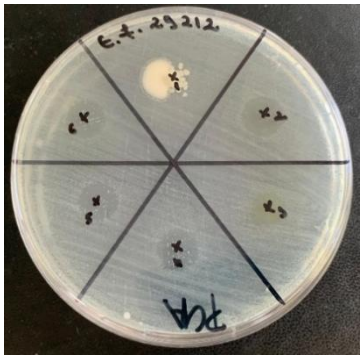

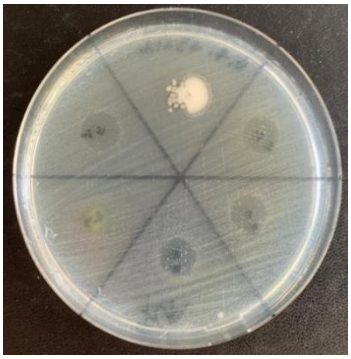

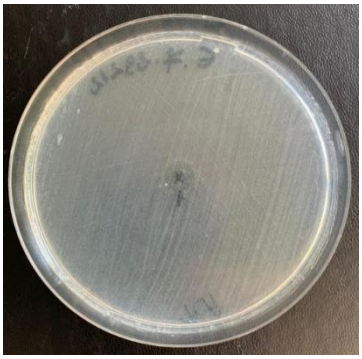

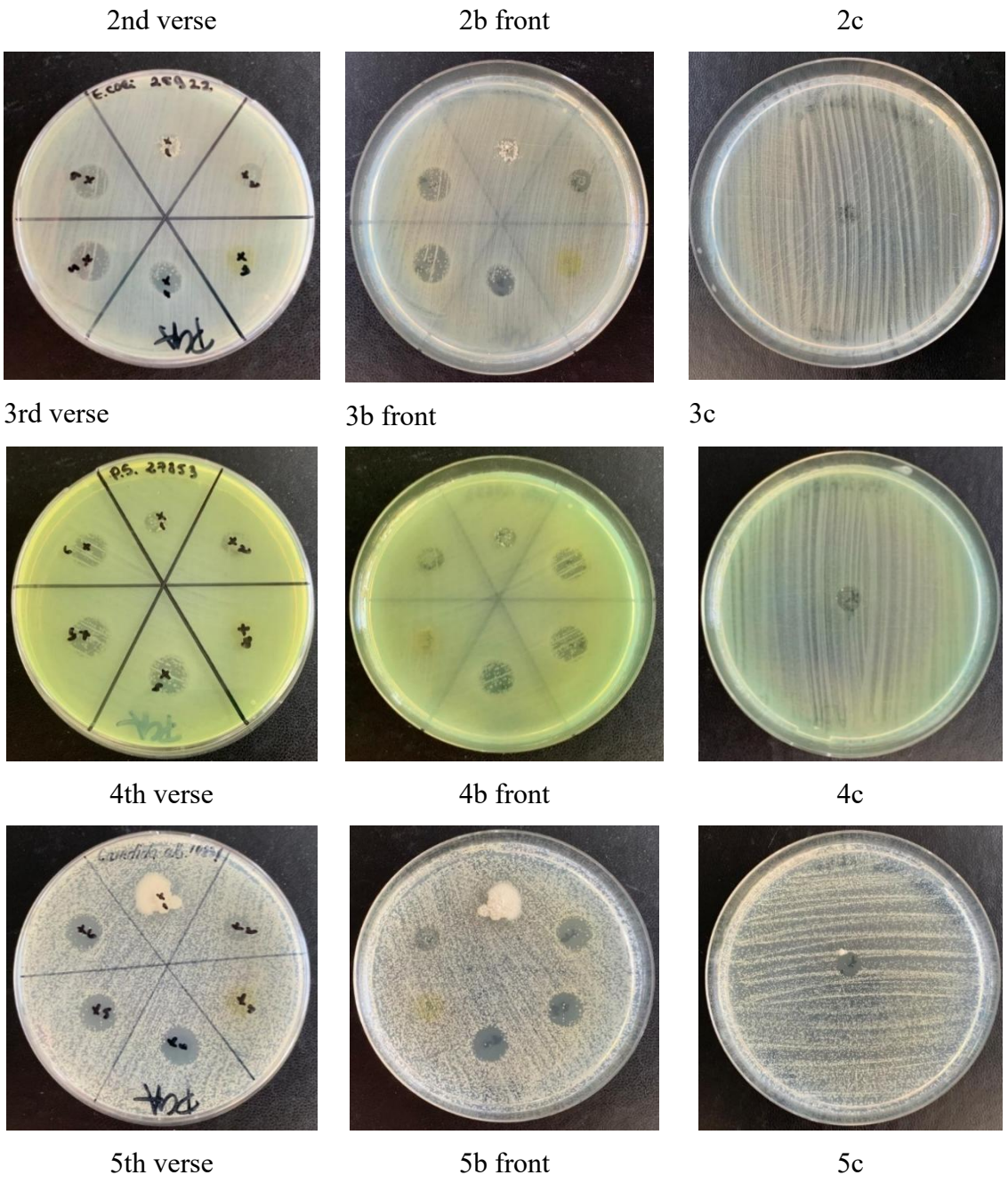

Face 1 Results of the qualitative evaluation of the antimicrobial activity of plant products for strains of S. aureus (position 1a,1b,1c), E. faecalis (position 2a,2b,2c), E.coli (position 3a,3b,3c), P. aeruginosa (position 4a,4b,4c) and C. albicans (position 5a,5b,5c) after incubation, 18-24h at 37ºC.

Table III Qualitative determination of the antimicrobial activity of plant products

Strain Tested	**Diameter of growth inhibition zone (mm)**			
	T. officinale **(tincture)**	***C. majus*** **(tincture)**	***S.marianum*** **(tincture)**	***A.annua*** **(alcoholic extract)**

				seed	Floweri ng	Before flowering
***S. aureus* ATCC 25923**	0	0	9∗	0	0	0
***E. faecalis* ATCC 29212**	9∗	11	8	10⁑	10⁑	10⁑
***E. coli* ATCC 25922**	0	7∗	0	9∗	11∗	10∗
***P.aeruginosa* ATCC 27853**	8∗	0	0	10∗	10∗	10∗
***C.albicans* ATCC 10231**	8⁑	7∗	0	11	11⁑	11⁑

Legend: ∗ Weak/slight microbial growth inside the inhibition zone.

⁑ the presence of a large number of colonies inside the inhibition zone.

4.3.5 RESULTS OF QUANTITATIVE DETERMINATION OF ANTIMICROBIAL ACTIVITY

The method of quantitative determination of antimicrobial activity allowed to highlight the concentrations of plant extracts at which the inhibition of growth and development of the tested reference strains occurs, as well as the concentrations that determine the bactericidal action.

Plant extract of *T. officinale* has a strong inhibitory effect on the Gram-negative strain *P. aeruginosa* ATCC 27853 and fungal, the bacteriostatic effect being achieved at the concentration of 3.13%, while on the Gram-positive strains and the *E. coli* ATCC 25922 the concentration of the plant extract required to inhibit microbial growth is 12.5-25%.

On the Gram-negative strains and the *strain E. faecalis* ATCC 29212, the concentration of 12.5% of the extract of *C. majus* has a bacteriostatic effect, thus being recorded a medium inhibitory effect, but a weak and strong inhibitory effect of this extract was observed on the strains *C. albicans* ATCC 10231 and *S. aureus* ATCC 25923, with CMI values of 50% and 3.13% respectively (Figure 10).

In the case of *S. marianum tincture*, the minimum concentrations that induced inhibition of bacterial growth and development for the strains *S. aureus* ATCC 25923, *E. faecalis* ATCC 29212, *E. coli* ATCC 25922, *P. aeruginosa* ATCC 27853 and *C. albicans* ATCC 10231 reached the values of 12.5%, 6.25%, 25%, 12.5% and 50% respectively (Figure 8).

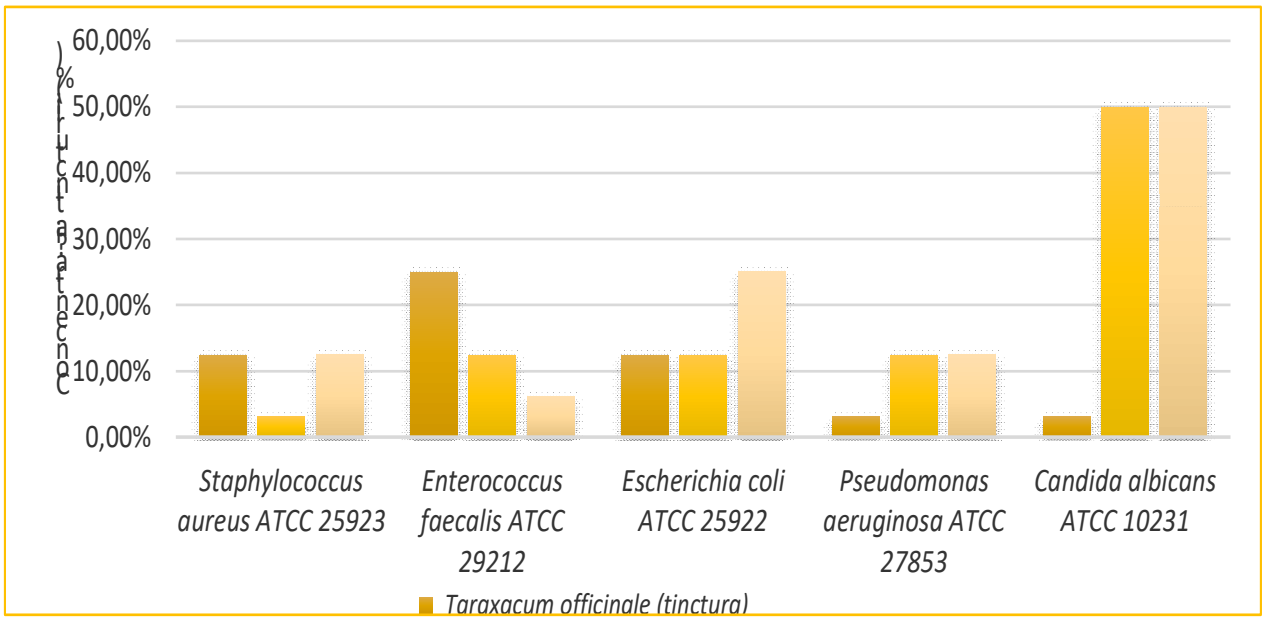

Face 2 Graphical representation of the minimum inhibitory concentration values of tinctures of T. officinale, C. majus and S. marianum, expressed in percentages

In the presence of the alcoholic extract of *A. annua* before flowering, inhibition of growth and development of Gram-positive strains was recorded at a concentration of 25%, and for Gram-negative strains and fungal strain it was observed at a concentration of 12.5%.

The highly antimicrobial activity of the alcoholic extracts of *A. annua* matura with seeds and during flowering was recorded in the presence of all the reference strains tested, the bacteriostatic effect for the strains *S. aureus* ATCC 25923, *E. faecalis* ATCC 29212, *E. coli* ATCC 25922 and *C. albicans* ATCC 10231 being achieved at C.M.I. values of 12.5%, 25%, 25% and 6.25% respectively.

The microbial activity of *P. aeruginosa* strain ATCC 27853 is inhibited in the presence of alcoholic extracts from *mature A. annua* with seeds and during flowering at concentrations of 12.5% and 6.25% (Figure 9).

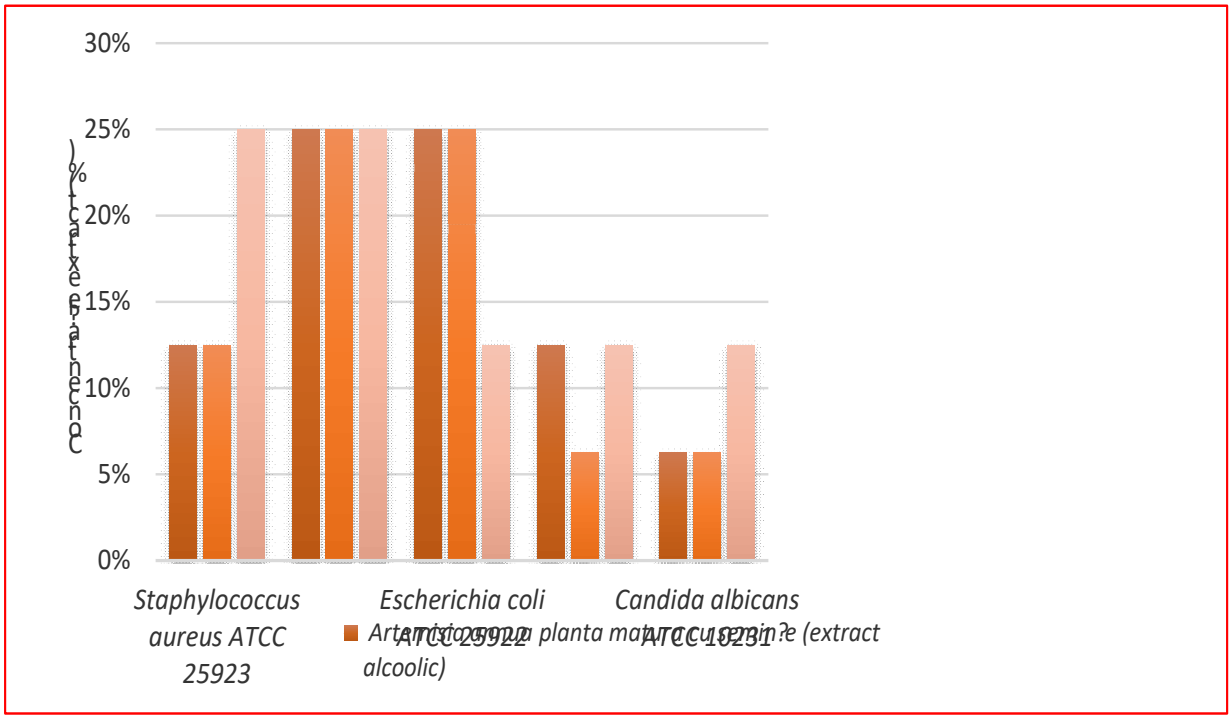

Face 3 Graphical representation of the values of the minimum inhibitory concentration of the alcoholic extracts of A. annua, expressed in percentages.

The tinctures tested in the study showed lethal action on the reference microbial strains at an average concentration of 20.8%. For the plant extract of *T. officinale* a concentration of 12.5% was required to obtain the bactericidal effect on the strains *S. aureus* ATCC 25923, *E. coli* ATCC 25922 and *C. albicans* ATCC 10231, and for the strains *E. faecalis* ATCC 29212 and *P. aeruginosa* ATCC 27853 concentrations of 50% and 6.25% respectively were required (Figure 10). In the presence of *C. majus* tincture, the lowest CMB value recorded was 6.25%, for the *S. aureus strain* ATCC 25923.

The bactericidal action on the strains *E. faecalis* ATCC 29212 and *P. aeruginosa* ATCC 27853 was observed at a concentration of 12.5% of the plant extract, while for the Gram-positive strain *E. coli* ATCC 25922 and the fungal strain, concentrations of 25% and 50%, respectively, were required.

Testing of the bactericidal action of *S. marianum* tincture reveals that a concentration of 12.5% is required to achieve this effect on Gram-negative strains and *P. aeruginosa* ATCC 27853, while for E. *coli strains* ATCC 25922 and *C. albicans* ATCC 10231 this effect is obtained at a much higher concentration of 50% (Figure 10).

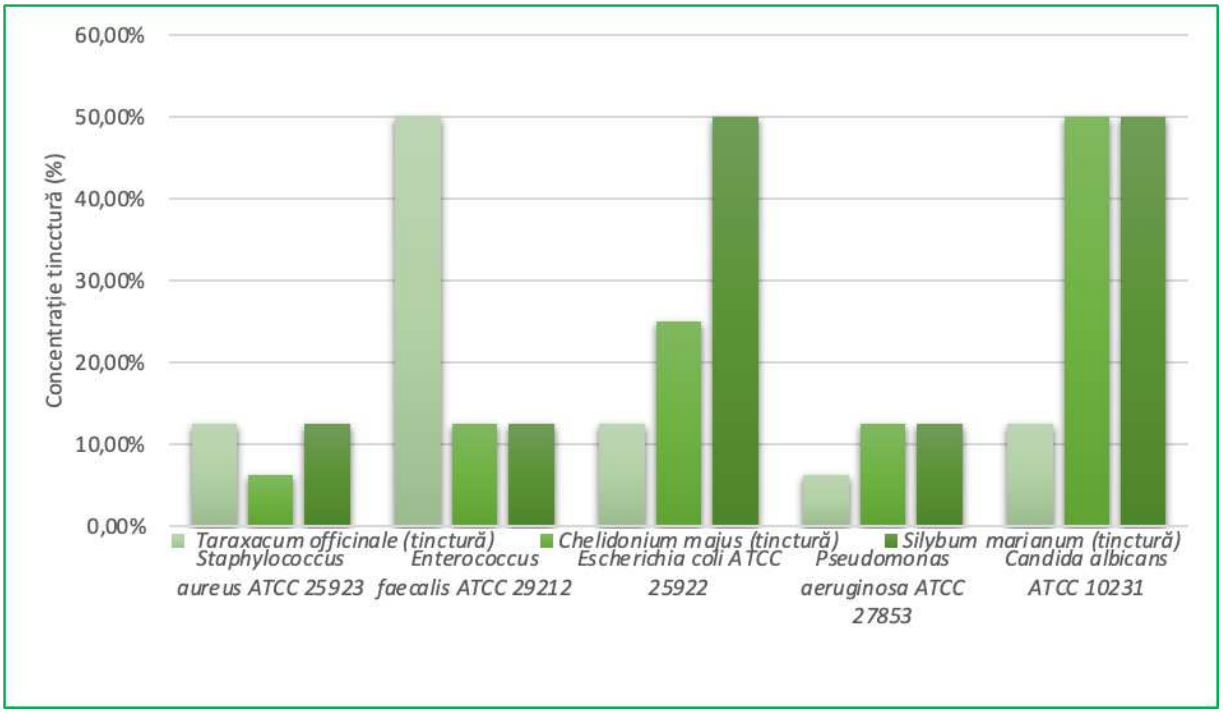

Face 4 Graphical representation of the values of the minimum bactericidal concentration of tinctures of *T. officinale, C. majus* and *S. marianum*, expressed in percentages

Through the analysis of the obtained results, the same efficiency was observed in terms of the concentration at which the bactericidal effect occurs for the alcoholic extracts of the mature seed plant and the plant during the flowering of *A. annua* (Figure 11).

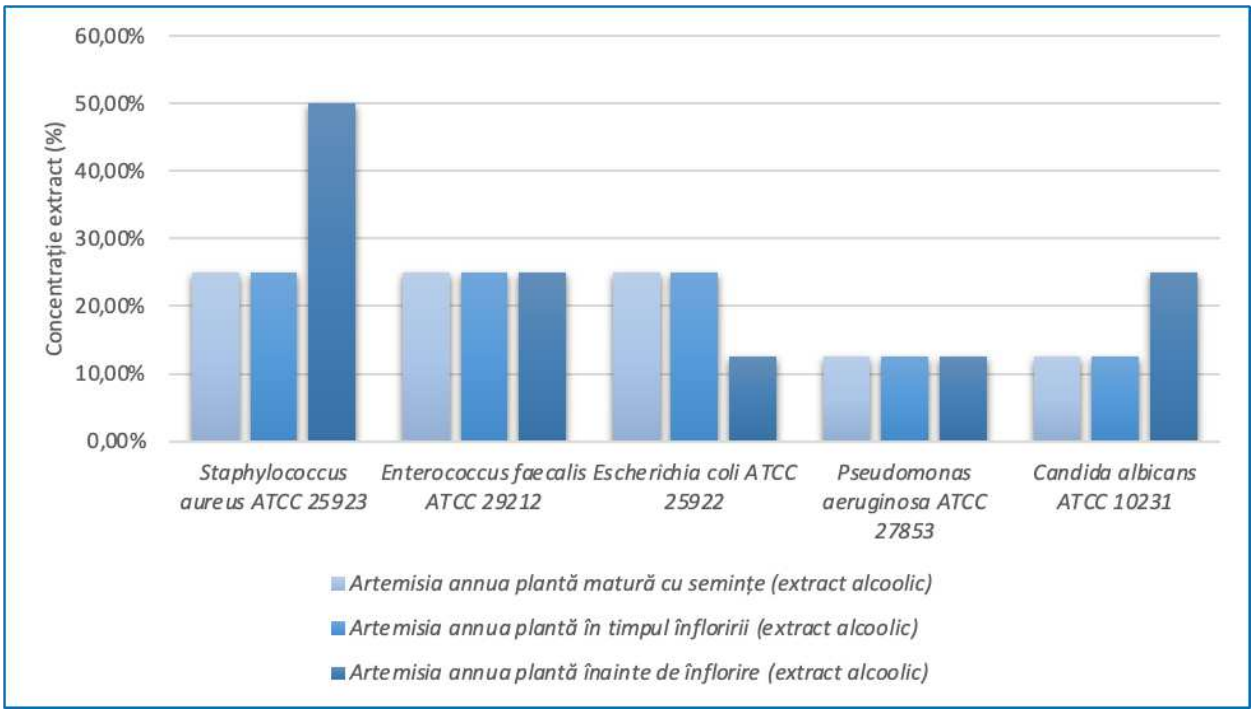

Face 5 Graphical representation of the values of the minimum bactericidal concentration of the alcoholic extracts of *A. per annum*, expressed in percentages.

They showed lethal action on the Gram-positive strains and the *E. coli strain* ATCC 25922 at a concentration of 25%, and for the fungal strain and *P. aeruginosa* ATCC 27853 the bactericidal effect was observed at a concentration of 12.5%. Under the conditions tested, the alcoholic extract from the pre-flowering plant *A. annua* exerts its bactericidal effect on the strains *E. faecalis* ATCC 29212 and *C. albicans* ATCC 10231 at a concentration of 25%, for the Gram-negative strains at a concentration of 12.5%, and for the strain of *S. aureus* ATCC 25923 a concentration of 50% was observed (Figure 12).

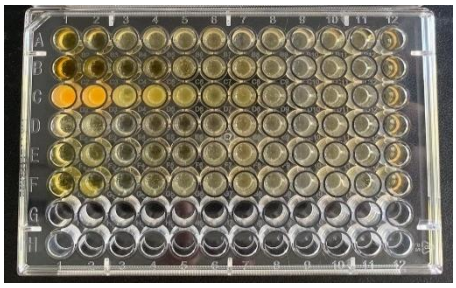

Staphylococcus aureus ATCC 25923

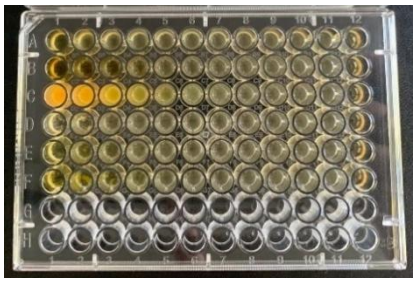

Enterococcus faecalis ATCC 29212

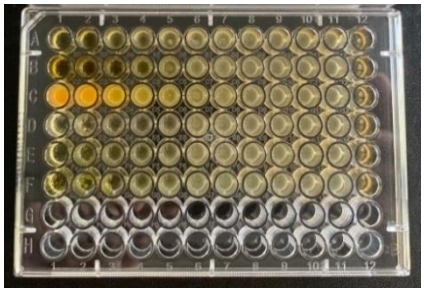

Escherichia coli ATCC 25922

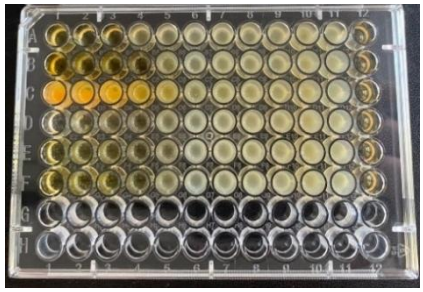

Pseudomonas aeruginosa ATCC 27853

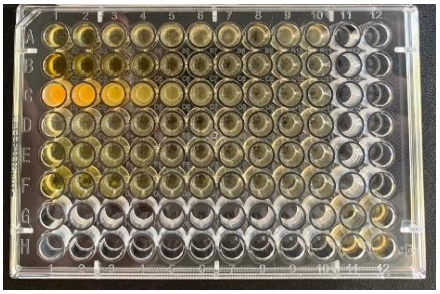

Candida albicans ATCC 10231

Figure 6 Results of the quantitative determination of the antimicrobial activity of plant products by the microdilution method. Microplates with 96 wells sown with *S. aureus*, *E. faecalis*, *E.coli, P. aeruginosa* and *C. albicans* developed in the presence of plant extracts, after incubation 18-24h at 37ºC.

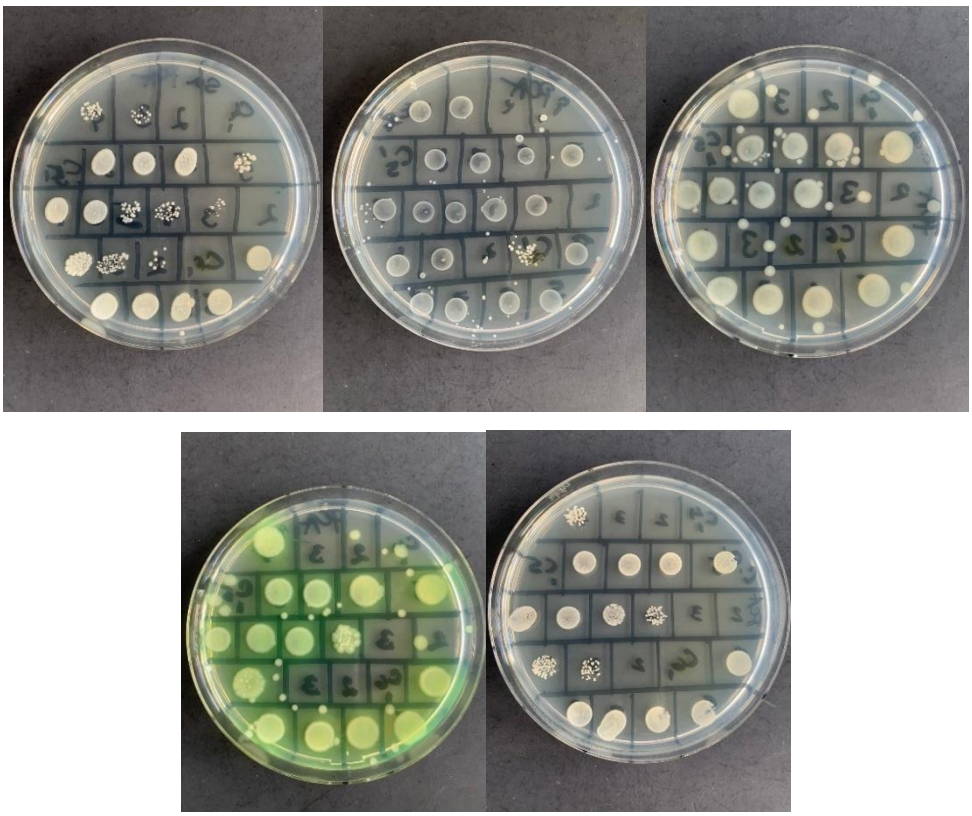

Figure 7 Antimicrobial activity test results. Agaric medium, seeded in a drop from microplates with 96 wells with stems of *S. aureus*, *E. faecalis*, *E.coli, P. aeruginosa* and *C. albicans*, after incubation for 18-24 hours at 37ºC.

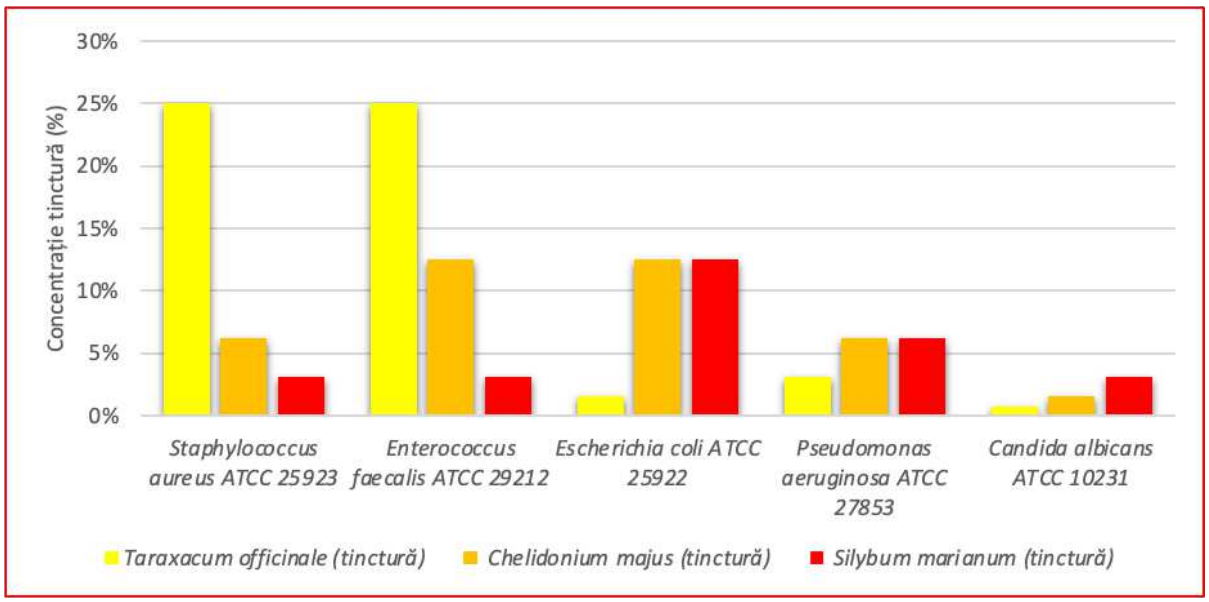

Figure 8 Graphical representation of the values of the minimum inhibitory concentration of tinctures of *T. officinale, C. majus* and *S. marianum* for inhibiting the development of biofilms, expressed in percentages.

4.3.6 RESULTS OF IN *VITRO ASSESSMENT* OF ANTIBIOTIC ACTIVITY

Analysis of spectrophotometric data revealed that *T. officinale* tincture has little effect on Gram-positive strains, inhibiting biofilm development at a concentration of 25%. The effect of this tincture was more increased on Gram-negative and fungal strains, with an inhibition of biofilm development being observed at concentrations of 0.78%, 1.56% and 3.13% for *C. albicans* ATCC 10231, *E. coli* ATCC 25922 and *P. aeruginosa* ATCC 27853 respectively (Figure 16).

The antibiofilm activity of the plant extract of *S. marianum* was reached at a minimum concentration of 3.13% for the Gram-positive bacterial and fungal strains, and for the Gram-negative strains *E. coli* ATCC 25922 and *P. aeruginosa* ATCC 27853 minimum concentrations of 12.5% and 6.25% were recorded.

The minimum concentration of *C. majus* tincture required to inhibit the biofilm development of the *C. albicans* strain ATCC 10231 is 1.56%, while for *E. faecalis* ATCC 29212 and *E. coli* ATCC 25922 the antibiofilm activity was achieved at a concentration of 12.5%, and for *S. aureus* ATCC 25923 and *P. aeruginosa* ATCC 27853 at 6.25% (Figure 15).

In the presence of all the alcoholic extracts of *A. annua* used in this study, the inhibition of bacterial biofilm development for the *strains E. faecalis* ATCC 29212 and *E. coli* ATCC 25922 was achieved at a minimum concentration of 12.5%, and for the fungal strain a higher efficacy of these three extracts was observed, the antibiofilm action being recorded at a minimum concentration of 1.56% (Figure 15).

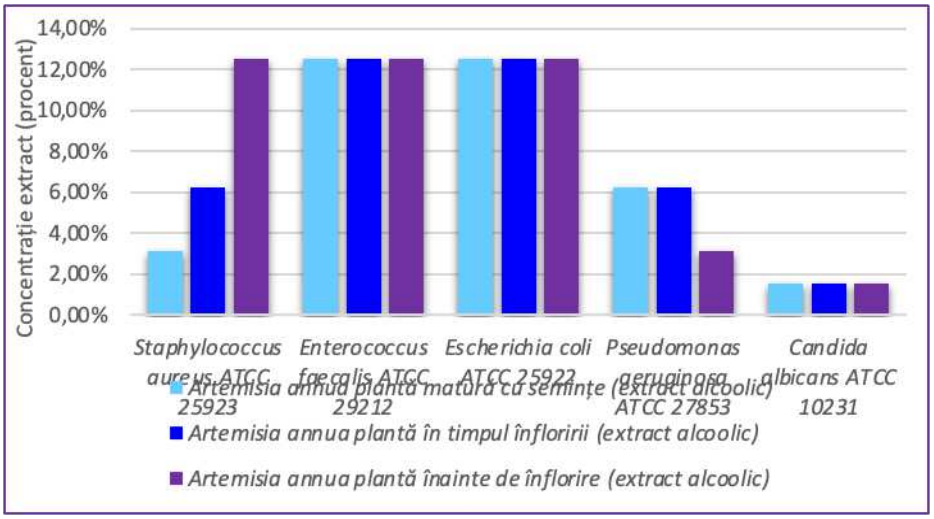

Face 9 Graphical representation of the values of the minimum biofilm inhibition concentration of alcoholic extracts of *A. annual*, expressed in percentages.

The alcoholic extract from *A. annual* mature seed showed an inhibition of biofilm development at a concentration of 3.13% for the *S. aureus*ATCC 25923 and 6.25% for *P. aeruginosa* ATCC 27853. Development of bacterial biofilm in the presence of alcohol extract from *A. annual* during flowering of the stems of *S. aureus*ATCC 25923 and *P. aeruginosa* ATCC 27853

was inhibited at a minimum concentration of 6.25%, and in the presence of the alcoholic extract from *A. annual* before flowering, values of 12.5% and 3.13% were recorded, respectively (Figure 16).

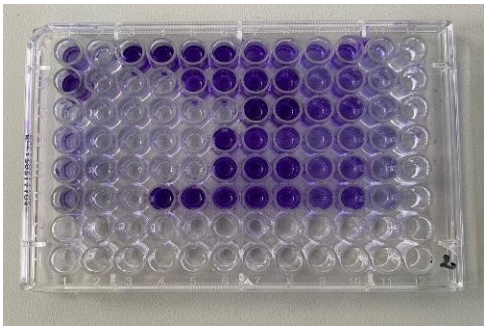

S. aureus ATCC 25923

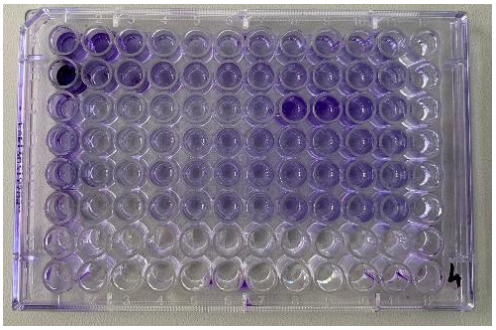

E. faecalis ATCC 29212

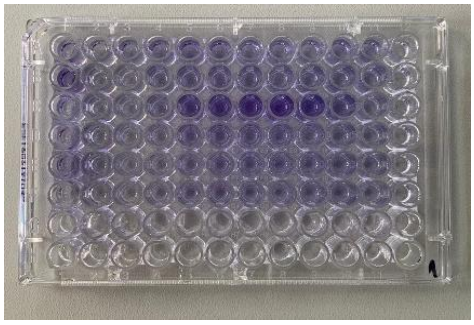

E. coli ATCC 25922

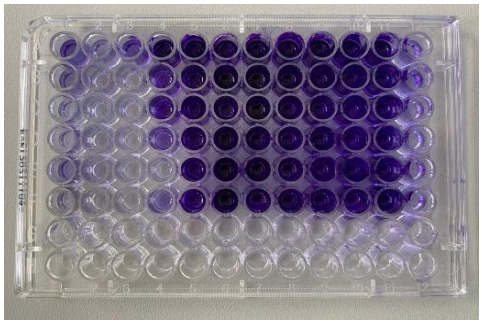

P. aeruginosa ATCC 27853

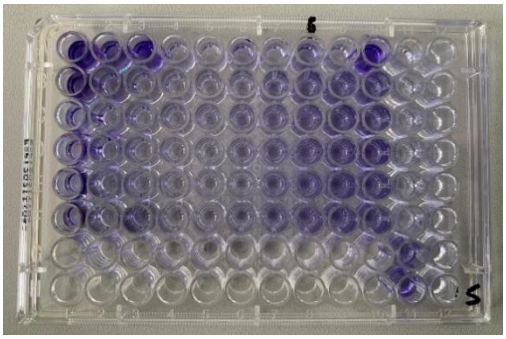

C. albicans ATCC 10231

Figure 10 Results of the determination of the antibiofilm activity of the tested plant extracts - the appearance of plates with 96 wells after solubilization with 33% acetic acid.

4.4 Conclusions

The highest free radical absorption capacity was observed in ***Artemisia annua*** **(65.44%),** followed closely by ***Taraxacum officinale*** **(59.34%).** On the other hand, ***Silybium marianum*** **(21.30%)** showed the lowest antioxidant capacity among the plants tested, followed by ***Chelidonium majus*** **(27.13%)**. Despite their lower antioxidant capacity in this test, these plants are known for other pharmacological properties.

White willow **(40.54%)** demonstrated moderate antioxidant capacity, which could be associated with its well-documented presence of phenolic glycosides, flavonoids, and tannins. The

results indicate a significant variability in the activity of free radical absorption among the plant species analyzed.

In addition, the antimicrobial properties of 6 plant extracts of *Taraxacum officinale* (tincture), *Chelidonium majus* (tincture), *Silybum marianum* (tincture) and *Artemisia annua* (alcoholic extract from mature plant with seeds; alcoholic extract from the plant during flowering; alcoholic extract from the plant before flowering) on 5 reference bacterial strains, two Gram-positive (*Staphylococcus aureus* ATCC 25923 and *Enterococcus faecalis* ATCC 29212), two Gram-negative (*Escherichia coli* ATCC 25922 and *Pseudomonas aeruginosa* ATCC 27853) and one fungal strain, *Candida albicans* ATCC 10231.

Qualitative testing of antimicrobial activity showed that the plant extracts inhibited the growth and development of the microbial strains tested, the tincture of *S. marianum* having a greater antimicrobial effect than the Gram-positive strains tested, while the alcoholic extracts of *A. anuua* exhibit a broad-spectrum antimicrobial action, being active against all microbial reference strains tested, except *S. aureus* ATCC 25923.

The quantitative determinations of the antimicrobial activity allowed to establish the concentrations of plant extracts responsible for the bacteriostatic and bactericidal effect, and a higher sensitivity of the microbial strains in the presence of tinctures can be observed compared to the presence of alcoholic extracts of *A. annua.*

The *in vitro* evaluation of the antibiofilm activity of the plant products showed their ability to inhibit the development of biofilms in the inert substrate; plant extracts of *C. majus*, *S. marianum* and *A. annua* were determined to inhibit the formation of biofilms in all bacterial strains tested, while *T. officinale* tincture showed very good activity on Gram-negative and fungal strains.

The results obtained are promising, supporting closer research of the biochemical characteristics of these extracts, in order to formulate strategies for the control of bacterial and fungal infections in humans.

The results of this chapter were published in the following articles:

1. **Daniel Cord**, Mirela Claudia Rimbu, Liliana Popescu, *New prospects in oncotherapy: bioactive compounds from Taraxacum officinale*, Medicine and Pharmacy Reports, https://doi.org/10.15386/mpr-2875

5. ADVANCED ANTIMICROBIAL AND ANTITUMOR DRUG DELIVERY SYSTEMS: GOLD AND SILVER NANOPARTICLES ACHIEVED BY GREEN SYNTHESIS WITH BIOACTIVE COMPOUNDS FROM PLANT EXTRACTS

5.1 INTRODUCTION

In the current context marked by the alarming increase in infections with multidrug-resistant bacteria, medicinal plants represent a promising source of bioactive compounds with antimicrobial, anti-inflammatory and antioxidant potential. The use of plant extracts for the synthesis of nanoparticles by green methods has attracted significant interest in recent decades.

The plants studied – *Taraxacum officinale* (dandelion), *Artemisia annua* (pelinita), *Melisa officinalis* (lemon balm) and *Salix alba* (willow) – are recognized for their multiple therapeutic applications in traditional and modern medicine. The active compounds extracted from them exhibit antioxidant, antibacterial, antifungal, and even antitumor properties.

The general aim of this study was the ecological synthesis of nanoparticles from plant extracts (*Melissa officinalis, Artemisia annua, Salix alba*) and the evaluation of their therapeutic, pharmaceutical and antimicrobial potential through advanced physicochemical and biological characterization methods. At the same time, the study aimed to investigate the synergistic effects of nanoparticles derived from *Melissa officinalis* in association with conventional chemotherapy agents used in the treatment of liver carcinoma, in order to develop effective systems for the administration of antitumor therapy.

5.2 MATERIALS AND METHODS

5.2.2 NANOPARTICLE SINTEZA *GREEN*

5.2.2.1 SYNTHESIS OF DIN NANOPARTICLES OBTAINED FROM SALIX ALBA EXTRACT

The formation of Ag-NPs during biosynthesis was confirmed by changing the color of the solution from yellow to dark brown after the addition of 18 mL of *Salix alba extract.* A unique property of spherical Ag-NPs is that wavelengths in plasma surface resonance (SPR) can be changed from 400 nm (violet light) to 530 nm (green light) by changing the particle size and refractive index near the particle surface [240].

To determine the Ag-NP sizes, UV-Vis spectrometry was used to record their wavelengths and correlate them with the size of the nanoparticles obtained after their synthesis. The UV-Vis absorption and maximum wavelength of Ag-NP are given by the size, shape, and medium in which they are dispersed, the density of free electrons, and their interactions with other chemical compounds in the environment [241].

5.2.2.3 SYNTHESIS OF ARTEMISIA ANNUA NANOPARTICLES

Similarly, the gold nanoparticles were obtained using only the aqueous wormwood extract. The gold nanoparticles obtained from the aqueous wormwood extract have been abbreviated as AuNPsEaqSW.

5.2.2.4 SYNTHESIS OF MELISSA OFFICINALIS NANOPARTICLES

The synthesis was verified visually, by changing the color of the solution, and the samples were collected for UV-Vis spectroscopic analysis, confirming the formation of the nanoparticles.

5.2.5.METHODS FOR ASSESSING THE ANTIMICROBIAL EFFECT

5.2.5.1. Evaluation of the antimicrobial effect of Salix alba extract and the resulting nanoparticles

Representative species for the main groups of pathogenic bacteria (the most common in human and veterinary infectious pathology, in hospital flora, in nosocomial infections and in multidrug-resistant infections) were chosen: *Staphylococcus aureus* (*S.a*), for gram-positive cocci; *Escherichia coli* (*E.c*), for gram-negative bacilli, enterobacteriaceae; *Pseudomonas aeruginosa* (*P.a*), for gram-negative, non-enterobacteriaceae bacilli.

	1	2	3	4	5	6	7	8	9	10	11	12	SAMPLES		
													Nanoparticles	Hydrogels	Ointments (Ont)
A	PS 200 µl	MHB: 100 µl PS: 50 µl S1-D1: 50 µl	MHB: 100 µl PS: 50 µl Bacteria: 50 µl	MHB: 100 µl Bacteria: 50 µl S1-D1: 50 µl	Idem 4	Idem 4	MHB: 100 µl Bacteria: 50 µl S1-D2: 50 µl	Idem 7	Idem 7	MHB: 100 µl Bacteria: 50 µl S1-D3: 50 µl	Idem 10	Idem 10	SAuNPs-WT 1S	Hydrogels Control	Tween 20
B	PS 200 µl	MHB: 100 µl PS: 50 µl S2-D1: 50 µl	MHB: 100 µl PS: 50 µl Bacteria: 50 µl	MHB: 100 µl Bacteria: 50 µl S2-D1: 50 µl	Idem 4	Idem 4	MHB: 100 µl Bacteria: 50 µl S2-D2: 50 µl	Idem 7	Idem 7	MHB: 100 µl Bacteria: 50 µl S2-D3: 50 µl	Idem 10	Idem 10	SAgNPs-WT 1S	AgNO3+PVP+PEG	Ont 1+SAgNPs-WT 10S+1% tween 20
C	PS 200 µl	MHB: 100 µl PS: 50 µl S3-D1: 50 µl	MHB: 100 µl PS: 50 µl Bacteria: 50 µl	MHB: 100 µl Bacteria: 50 µl S3-D1: 50 µl	Idem 4	Idem 4	MHB: 100 µl Bacteria: 50 µl S3-D2: 50 µl	Idem 7	Idem 7	MHB: 100 µl Bacteria: 50 µl S3-D3: 50 µl	Idem 10	Idem 10	Salix alba Extract	Hydrogel A	Ont 1+SAgNPs-WT 10S+1% tween 20 (1:1:1)
D	PS 200 µl	MHB: 100 µl PS: 50 µl S4-D1: 50 µl	MHB: 100 µl PS: 50 µl Bacteria: 50 µl	MHB: 100 µl Bacteria: 50 µl S4-D1: 50 µl	Idem 4	Idem 4	MHB: 100 µl Bacteria: 50 µl S4-D2: 50 µl	Idem 7	Idem 7	MHB: 100 µl Bacteria: 50 µl S4-D3: 50 µl	Idem 10	Idem 10	Salix alba Extract	AgNO3+PVP+Gly	Ont 1+SAgNPs-WT 10S+1% tween 80 (1:1:1)
E	PS 200 µl	MHB: 100 µl PS: 50 µl S5-D1: 50 µl	MHB: 100 µl PS: 50 µl Bacteria: 50 µl	MHB: 100 µl Bacteria: 50 µl S5-D1: 50 µl	Idem 4	Idem 4	MHB: 100 µl Bacteria: 50 µl S5-D2: 50 µl	Idem 7	Idem 7	MHB: 100 µl Bacteria: 50 µl S5-D3: 50 µl	Idem 10	Idem 10	SAuNPs-WT 7S	Hydrogel B	Ont 2+SAgNPs-WT 10S+1% tween 80
F	PS 200 µl	MHB: 100 µl PS: 50 µl S6-D1: 50 µl	MHB: 100 µl PS: 50 µl Bacteria: 50 µl	MHB: 100 µl Bacteria: 50 µl S6-D1: 50 µl	Idem 4	Idem 4	MHB: 100 µl Bacteria: 50 µl S6-D2: 50 µl	Idem 7	Idem 7	MHB: 100 µl Bacteria: 50 µl S6-D3: 50 µl	Idem 10	Idem 10	SAuNPs-WT 10S	AgNO3+PEG_Gly	Ont 2+SAgNPs-WT 10S+1% tween 20 (1:1:1)
G	PS 200 µl	MHB: 100 µl PS: 50 µl S7-D1: 50 µl	MHB: 100 µl PS: 50 µl Bacteria: 50 µl	MHB: 100 µl Bacteria: 50 µl S7-D1: 50 µl	Idem 4	Idem 4	MHB: 100 µl Bacteria: 50 µl S7-D2: 50 µl	Idem 7	Idem 7	MHB: 100 µl Bacteria: 50 µl S7-D3: 50 µl	Idem 10	Idem 10	SAgNPs-WT 7S	Hydrogel C	Ont 2+SAgNPs-WT 10S+1% tween 80 (1:1:1)
H	PS 200 µl	MHB: 100 µl PS: 50 µl S8-D1: 50 µl	MHB: 100 µl PS: 50 µl Bacteria: 50 µl	MHB: 100 µl Bacteria: 50 µl S8-D1: 50 µl	Idem 4	Idem 4	MHB: 100 µl Bacteria: 50 µl S8-D2: 50 µl	Idem 7	Idem 7	MHB: 100 µl Bacteria: 50 µl S8-D3: 50 µl	Idem 10	Idem 10	SAgNPs-WT 10S	AgNO3 1N	Tween 80

5.2.5.2. Evaluation of the activity effect of Artemisia annua extract

For antibacterial activity, selected opportunistic pathogenic bacterial strains, namely *Staphylococcus aureus* a Gram-positive coccus; *Escherichia coli,* a *Gram-negative bacillus,*

family Enterobacteriaceae; Pseudomonas aeruginosa, a Gram-negative *bacillus*, from the *non-Enterobacteriaceae family,* and *Bacillus subtilis,* a *Bacillaceae bacillus*

For antifungal activity, several species of emerging fungal pathogens were tested, including yeasts, such as *Saccharomyces cerevisiae*, *Candida albicans, and* filamentous fungi such as *Penicillium sp*. and *Aspergillus sp.*, using a Sabouraud Agar medium.

The potential cytotoxic activity of the studied extracts was evaluated on two standardized adherent human cancer cell lines against normal human endothelial cells and compared with the cytotoxicity of oncology drugs commonly used for cancer treatment.

5.2.6 Methods for assessing the antitumor (antiproliferative) effect

5.2.6.1 Evaluation of the antiproliferative activity of Salix alba extract and synthesized nanoparticles

Cell viability was determined using the MTT colorimetric assay (3-(4,5-dimethylthiazole-2-yl)-2,5-diphenyltetrazolium bromide). After treatment, the cells were incubated for 24 and 48 hours, respectively, with different concentrations (5, 10, 25, 50 and 100 μg/mL) of nanoparticles [50]. Subsequently, the growing medium was removed, and each well was washed with buffer solution

5.2.6.2. Evaluation of the antiproliferative activity of Artemisia annua extract and synthesized nanoparticles

The potential cytotoxic activity of studied pelinite extracts was evaluated on two standardized adherent human cancer cell lines against normal human endothelial cells and compared with the cytotoxicity of oncology drugs commonly used for cancer treatment.

5.2.6.3 Evaluation of the antiproliferative activity of Melisa officinalis extract and synthesized nanoparticles

The cytotoxic potential of the investigated plant extracts, their combination with nanoparticles, antitumor drugs and anticancer drugs used as control groups (sunitinib and imatinib) was evaluated on a standardized, adherent human cancer cell line, and compared with the effects on normal human endothelial cells, using an oncolytic drug commonly used in cancer therapy as a standard.

Human hepatic adenocarcinoma cell line (HepG2, HB-8065) and human umbilical vein endothelial cells (HUVEC, CRL-1730) were obtained from the **American Type Culture Collection** (ATCC, Manassas, WV, USA). Sunitinib 50 mg capsules (Sunitinib® — Accord, Barcelona, Spain) and Imatinib 100 mg tablets (Imakrebin® — Alvogen, Luxembourg) were used as classical anticancer agents for the treatment of cell control groups. The working solutions were freshly prepared for each experiment by serial dilutions of the stock solutions in the culture medium.

5.3. RESULTS AND DISCUSSIONS

5.3.1 PHYSICOCHEMICAL CHARACTERIZATION OF NANOPARTICLES

5.3.1.1 OPTICAL AND STRUCTURAL CHARACTERIZATION OF NAOPARTICLES OBTAINED FROM SALIX ALBA BY UV-VIS, FLUORESCENCE AND X-RAY DIFFRACTION

The phytochemical compounds in *Salix alba bark extract* were silver reducers and stabilizers, and the addition of repeated volumes of the extract resulted in an increase in the concentration of silver nanoparticles.

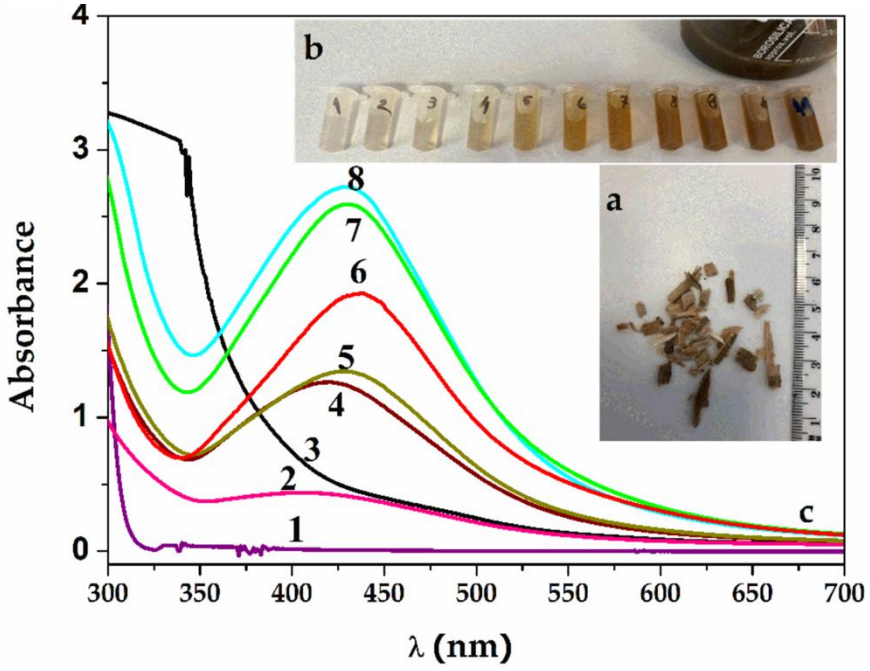

Face 11 (**a**) Bark of*Salix alba L.*was collected in Dâmbovița County, Romania, from willow trees. (**b**) Change the colour of the solution from yellow to dark brown. (**c**) UV-Vis spectra of SAgNP-WT samples obtained by time reduction with aqueous willow extract:$_{1\text{-}AgNO3}$0,5 mM; 2-SAgNPs-WT 1S (după 5 min); 3-extract de salcie; 4-SAgNPs-WT 4S (după 10 min); 5-SAgNPs-WT 5S; 6-SAgNPs-WT 7S; 7-SAgNPs-WT 9S; și 8-SAgNPs-WT 10S.

The spectra in Figure 18c represent the occurrence of an initial absorption maximum after 5 min of reaction at a wavelength of 409 nm (spectra 2), manifesting as a widening band and thus showing a polydispersion of the silver nanoparticles formed. This band narrows and reaches a wavelength of 420 nm after 10 minutes (4 spectra).

The stability of SAgNPs-WT was also evaluated spectrophotometrically one year after synthesis. The UV-Vis spectra shown in Figure 19 show no noticeable changes in the maximum absorption band after storing the solutions for one year at room temperature.

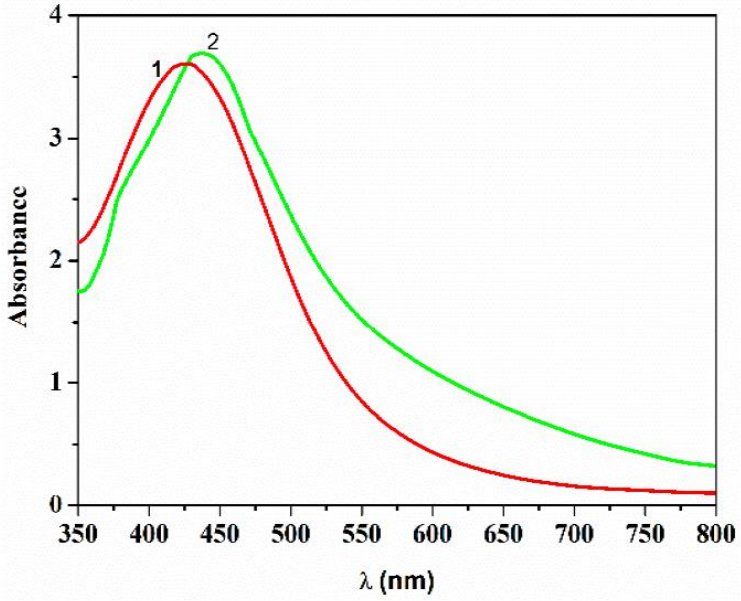

Face 12 UV-VIS spectra of: Initial colloidal solution with SAgNPs-WT; 2. After one year of storage at room temperature sheltered from light

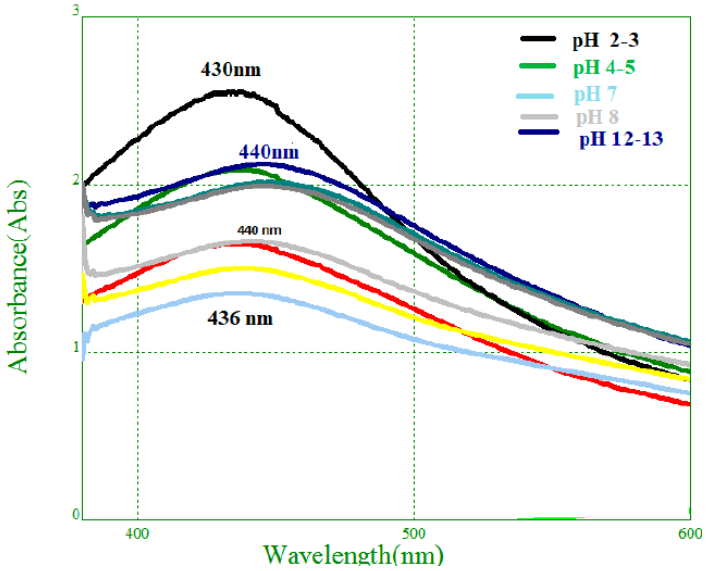

Face 13 UV-Vis spectra showing the effect of pH variation on the stability of SAgNPs-WT

The possibility of using SAgNPs-WT in environments with different pH has also been evaluated by UV-Vis characterization, Figure 31 showing the characteristic spectra of colloidal solutions with SAgNPs-WT modified by adjusting the pH with 1 M NaOH or 1 M HCl solutions. We can observe their stability in a pH range between 2 and 8; the bands begin to widen as the pH values increase. The solutions showed very good stability in acidic environments, but also did not show major changes in the initial wavelength when they had a slightly basic pH.

The presence of small amounts of amino acids was evidenced by the emission spectrum obtained at 280 nm, with a maximum at 312 nm, and by the excitation spectrum with a maximum at 276 nm, which are the characteristic bands of tyrosine Figure 21b.

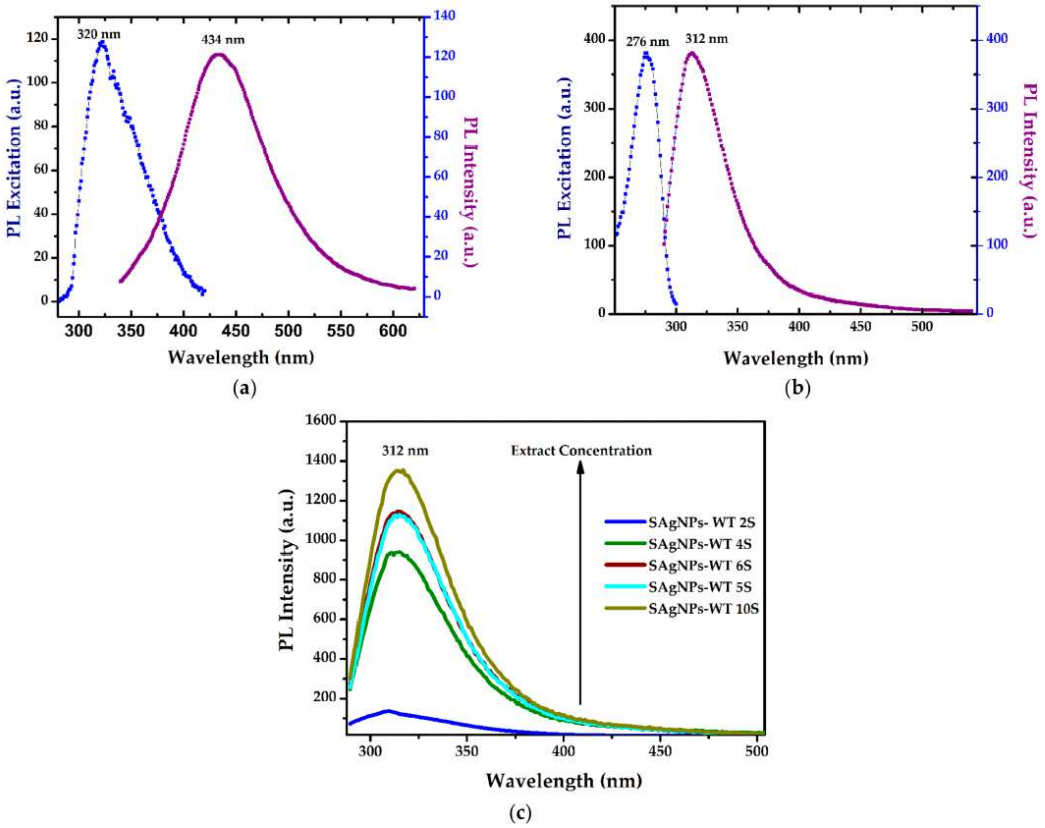

Face 14 Photoluminescence excitation (PLE) and emission (PL) spectra recorded for colloidal dispersion SAgNPs-WT at (a) 320 nm excitation; (b) tyrosine band characteristics at ex/em = 276/312 nm; and (c) the increase of the tyrosine band (312 nm) with the concentration of the extract during biosynthesis.

A slight redshift was identified compared to free tyrosine whose fluorescence is localized at λex/λem = 274/310 nm. In addition, the PL emission of eight samples of SAgNPs-WT extracted during synthesis at 3-5 minute intervals was analyzed and are shown in Figure 21c.

The intensity of the peak PL of 312 nm shows that the concentration of tyrosine increases significantly with the reaction time with the increase in the amount of extract added during synthesis. This may be another confirmation of the existence of polyphenolic compounds that exhibit fluorescence and whose fluorescence increases with the formation of silver nanoparticles.

Quantitatively, the decrease in peak width is correlated with an increase in the average size of crystallites, according to the Debye-Scherrer equation. A size of 5.67 nm was found for Au-NPs, while Ag-NPs showed larger average crystallite sizes (16.12 nm). The presence of XRD

peaks and average crystallite sizes of several nm indicate that the synthesized NPs were nanocrystalline.

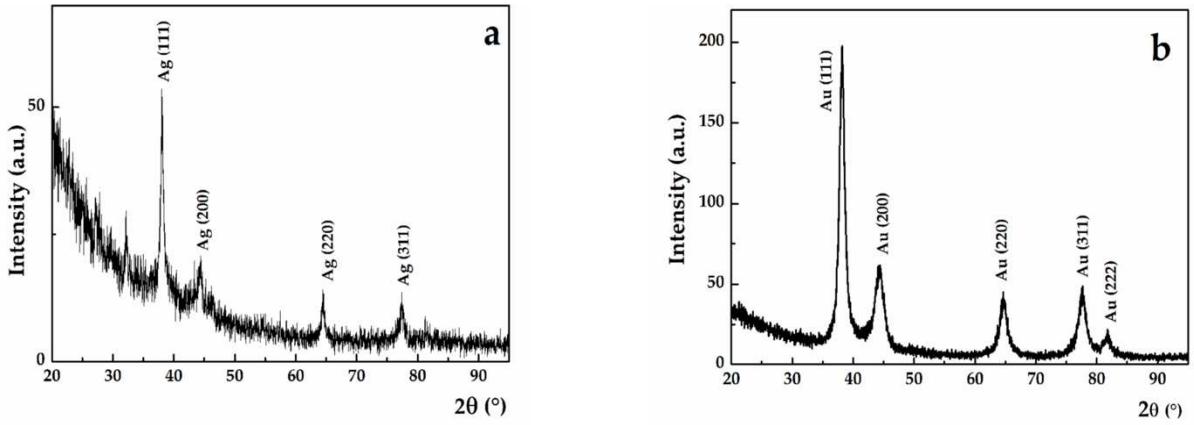

Face 15 Grazing incidence X-ray diffraction (GIXRD) model for (**a**) SAgNPs-WT and (**b**) SAuNPs-WT. Spikes were indexed according to the ICDD database

5.3.1.2 UV-VIS CHARACTERIZATION AND DETERMINATION OF POLYPHENOL CONTENT IN ARTEMISIA ANNUA-BASED SAMPLES, EXTRACTS AND NANOPARTICLES

UV-VIS spectrophotometric analysis monitored the formation of silver and gold nanoparticles reduced by *Aremisia annua* extracts. The absorption spectra of the extracts were recorded at 200-700 nm.

Figure 23 shows the UV-VIS spectra obtained for nanoparticle solutions formed by bioreduction with aqueous or alcoholic extracts. Figure 18(a) shows the UV-VIS spectra for silver nanoparticles reduced with the aqueous pelinite extract, AgNPSEaqSW(I), and the alcoholic extract, AgNPSEETOHSW(II). For gold nanoparticles from Artemisia annua, spectra are shown in Figure 1(b), with the aqueous extract indicated as AuNPSEaqSW (I) and the alcoholic extract as AuNPSEETOHSW (II).

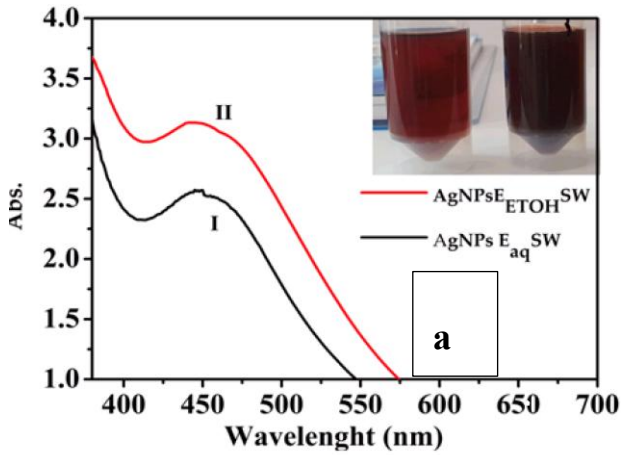

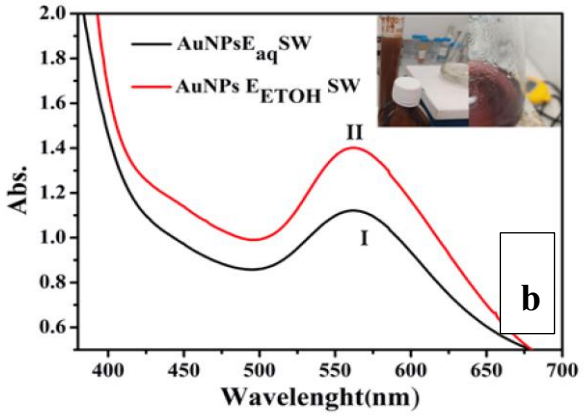

Face 16 UV-VIS spectra obtained for nanoparticle solutions formed by bioreduction with aqueous or alcoholic extracts

The bioreduction of the gold in the pellet resulted in the formation of a maximum absorbance at 563 nm for the EaqSW AuNPs, corresponding to a nanoparticle size of approximately 105.67 nm (Haiss equation), as shown in the spectra in Figure 18 being the UV-VIS spectra of the EETOHSW AuNPs, which has a maximum absorbance at 557 nm and a corresponding calculated size of 111.12 nm. The inset in Figure 23(b) shows a color change from brown to red-purple, confirming the formation of gold nanoparticles.

5.3.1.3 UV-vis characterization of Melissa oficinalis-based extract and nanoparticles

The change in the color of the solution from red-brown to dark brown confirms the reduction of silver ions by the *Melissa officinalis*. The UV-Vis spectrum (Figure 24) indicated an initial absorption peak at 453 nm, which stabilized at 440 nm after 30 minutes, indicating stable nanoparticle formation. The final volumetric ratio between $AgNO_3$ 0.5 mM and lemon balm extract was 3.2:1 (v:v).

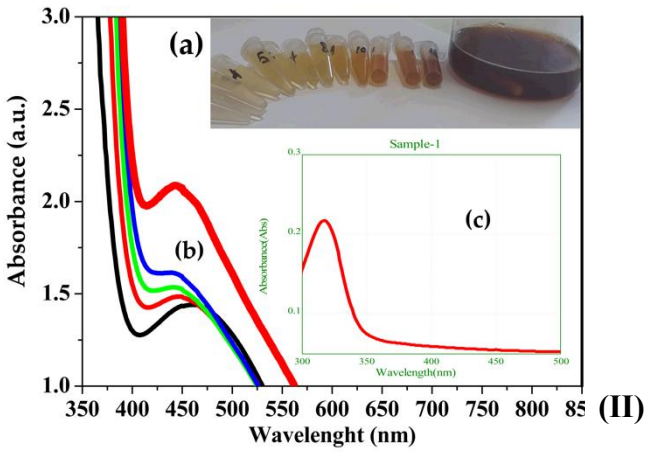

(I)

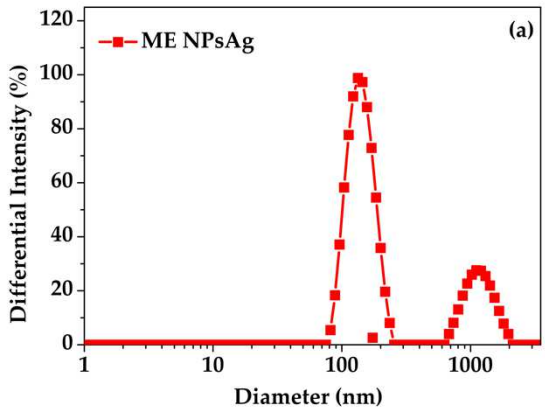

(II)

Face 17 The size distribution measured by DLS shown in Figure 24 showed two populations: Particles with sizes between 75 nm – 255 nm, with a maximum at 143 nm.

5.3.1.4 FTIR characterisation of Salix alba extract and nanoparticles

The ATR-FTIR spectra recorded for willow extract and SAgNPs-WT samples recorded at 1 day, 7 days, and 180 days after synthesis, respectively, are shown in Figure 25.

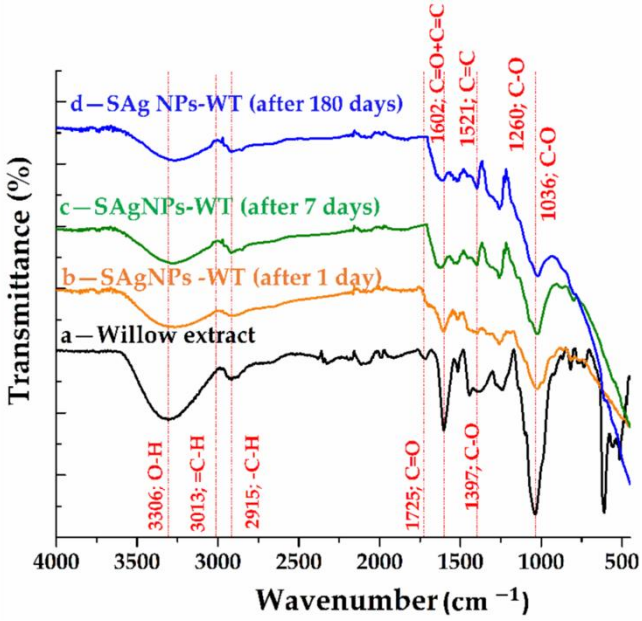

Face 18 ATR-FTIR spectra for (a) willow extract and silver nanoparticles, (b) 1 day, (c) 7 days and (d) 180 days after synthesis.

Comparing the spectra of the silver nanoparticle synthesis samples (Figure 25 b-d) with the spectrum of willow extract, a change in the spectrum below 700 cm-1 was observed, thus confirming the formation of Ag nanoparticles to which the willow clusters are anchored.

5.3.1.5 FTIR characterization of Salix alba formulations

The main structural composition of the raw materials (chitosan, gelatin and silver nanoparticles) and hydrogels containing silver nanoparticles, obtained according to the biogenic protocol presented above, can be deduced from the FT-IR spectra shown in Figure 26**.**

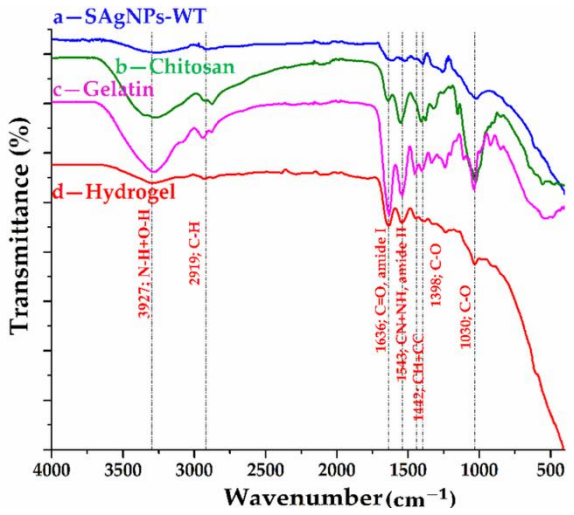

Face 19 ATR-FTIR spectra for (a) willow silver nanoparticles; (b) chitosan; (c) gelatin; and (d) silver nanoparticle hydrogel.

Depending on the process parameters, it has been found that gelatin and chitosan-based hydrogels can lead to different types of interactions (electrostatic, hydrogen bonds, Van der Waals, ionic or covalent), with the formation of a three-dimensional network due to gelatin. In the spectrum of the hydrogel shown in Figure 9, a mixture of bands characteristic not only of the amine groups of chitosan but also of the carboxyl groups of gelatin can be observed.

The interaction between silver nanoparticles and hydrogel components is supported by the displacement of bands that can be associated with C-O bonds in the carboxyl group (up to 1398, 1197, 1156 and 1030 $^{cm-1}$), as well as the lack of spectral bands below 900 [246,247].

5.3.1.6 FTIR characterisation of Artemisa annua-based extract and nanoparticles

Artemisia annua has as phytoconstituents, cis-epoxyocimene, cis-chrysanthemol, thuhona, bornyl or chrysanthenyl acetate, chrysanthemol, camazulene, sabinyl, 1,8-cineole, caryophyllene, mirene, junin, linalool, chrysanthemyl acetate and trans-sabinyl acetate can be isolated from pelinite.

5.3.1.7.1 Dimensional and morphological characterization of nanoparticles obtained from Salix alba by DLS, PDI, zeta potential, SEM and TEM

Hydrodynamic and electrophoretic light dispersion (DLS/ELS) measurements were performed to obtain information on hydrodynamic diameter (dh) and zeta potential (ζ) to predict the long-term stability of colloidal solutions SAg/AuNP-WT obtained after bioreduction in the aqueous extract of *Salix alba*.

The SEM images recorded for SAu/AgNPs-WT are shown in Figure 27 a,b for SAuNPs-WT and Figure 4 d,e for SAgNPs-WT, with spherical gold/silver nanoparticles with a mean size

distribution of 8-25 nm (mean size, 19.5 ± 0.7 nm) observed for SAuNPs-WT, while those for AgNPs-WT were larger, 10-38 nm (mean size, 21.5 ± 0.7 nm).

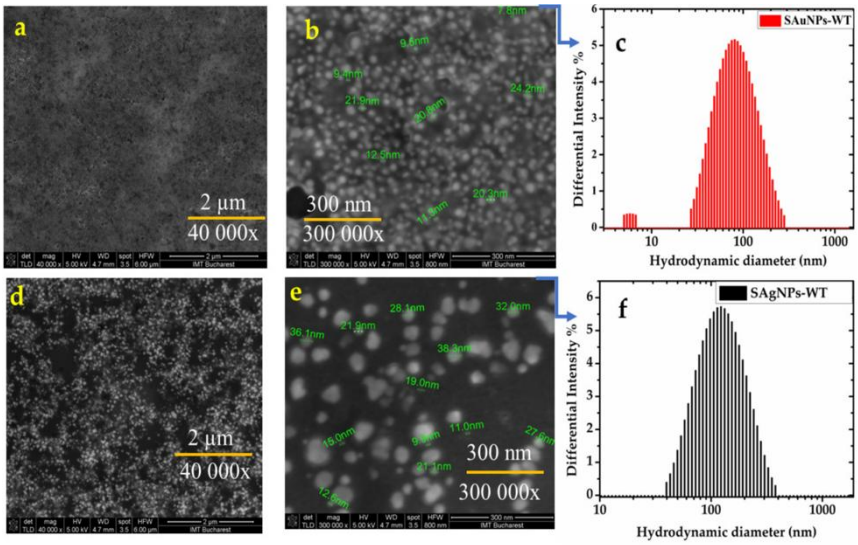

*Face 20 SEM images at different sizes and hydrodynamic diameters determined by DLS: (**a**)-SAuNPs-WT (40,000×); (**b**)-SAuNPs-WT (300,000×); (**c**)-DLS de SAuNPs-WT; (**d**)-SAgNPs-WT (40,000×); (**is**)-SAgNPs-WT (300,000×); and (**f**)-DLS de SAgNPs-WT.*

The histograms of the Ou/AgNPs-WT size distributions have been adjusted by Gaussian functions and are shown in Figure 28. The values obtained are consistent with previously collected data for *Salix alba* (gold/silver) nanoparticles extracted from its leaves and bark, respectively.

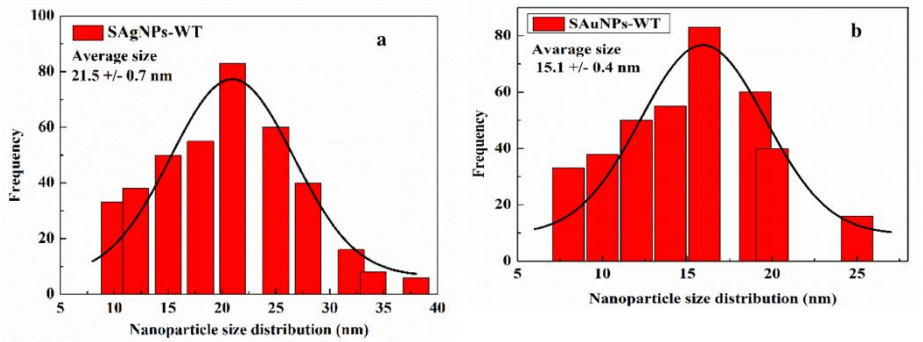

Face 21 (a)SAgNPs-WT distribution with N=389 and (b) SAuNPs-WT distribution with N=375

5.3.1.7.2 Hydrogel based on SAgNPs-WT

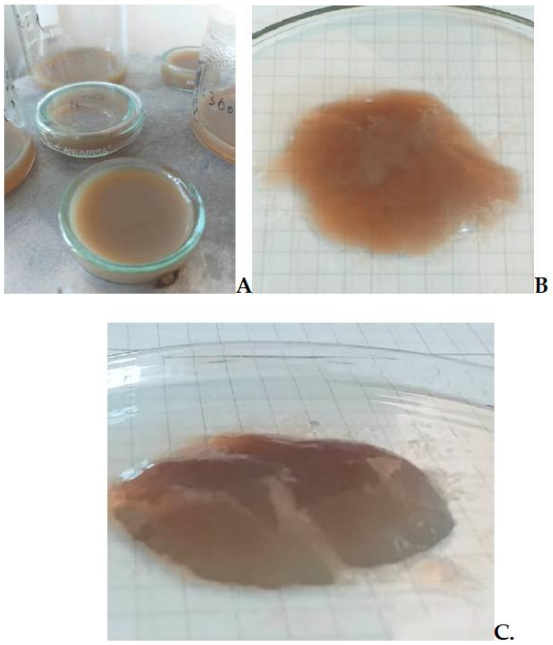

Face 22 Hydrogels with: A. chitosan-gelatin-SAgNPs-WT volume ratio = 3:7 and 5 mL SAgNPs-WT; B. ratio = 5:5 (v/v); C. ratio = 1:9

The hydrogels obtained were odorless, reddish-brown and homogeneous, as can be seen in Figure 29. The main advantage of the hydrogel, based on the green nanoparticles from Salix alba, is that a uniformity of SAgNPs-WT was achieved in its structure without the addition of an additional stabilizer. This can be confirmed in an SEM image in Figure 30, in which nanoparticles evenly distributed across polymer chain networks can be observed.

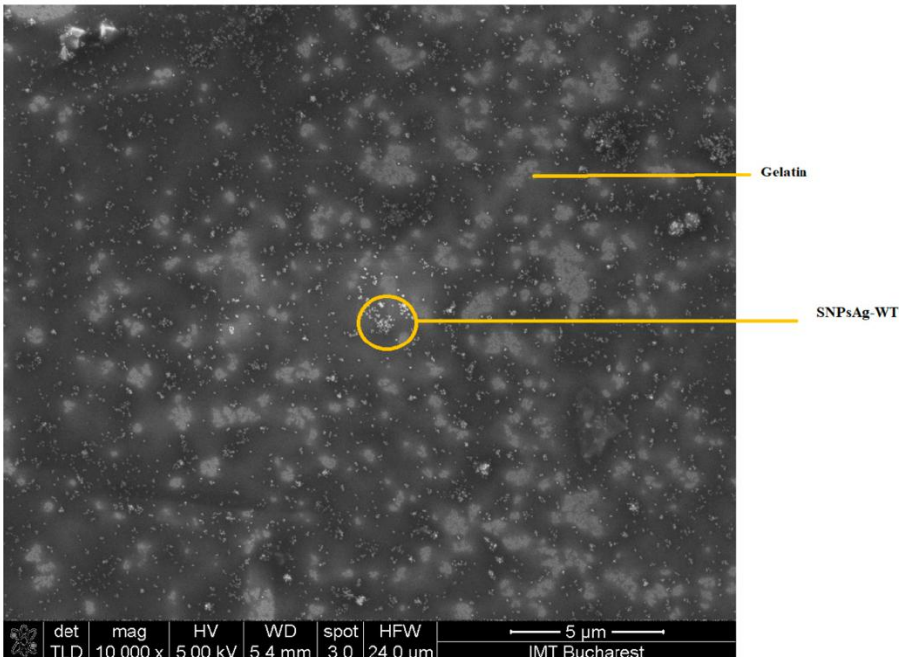

Face 23 SEM image of CS/G and SAgNPs-WT-based hydrogel

5.3.1.7.3 Dimensional and morphological characterization of Artemisa annua-based nanoparticles by DLS, PDI, zeta potential

The polydispersity index (PDI) represents the ratio of particles of different sizes to the total number of particles. A low PID value (<0.1) indicates a more monodisperse sample. The DLS spectra and the corresponding zeta potential for all samples are shown in Figure 31* (a1-d2) and Figure 32** (a1-d2).

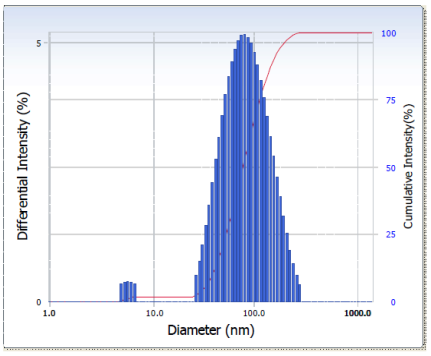

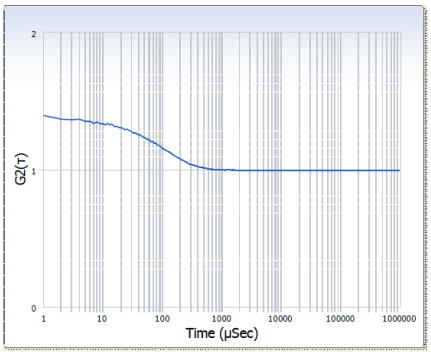

Distribution Results (Contin)

Peak	Diameter (nm)	Std. Dev.

Cumulants Results

Diameter	(d)	: 71.1	(nm)
Polydispersity Index	(P.I.)	: 0.267	

Figure S31*(a1) Hydrodynamic diameter, polydispersity index for AgNPsEaqSW

Version 3.73 / 2.30

Measurement Condition

Sampling Time	: 400	(µs)	Correlation Method	: TD	
Correlation Channel	: 512	(ch)	Accumulation times	: 10	(times)
Scattering Angle	: 15.0	(°)	Temperature	: 25.0	(°C)
Intensity	: 66084	(cps)	Attenuator 1	: 1.12	(%)
Cell Center	: X: 6.710	(mm)	Attenuator 2	: 4.420	(%)
	Z: 6.825	(mm)	Pinhole	: 50	(µm)
Cell Constant	: 105.530	(1/cm)			
Cell Type	: Flow Cell				
Apply Voltage Type	: NEGATIVE				

Electric Field

Avg. Electric Field	: -10.82	(V/cm)	Avg. Current	: -0.10	(mA)

Diluent Properties

Diluent Name	: WATER		Dielectric Constant	: 78.2	
Refractive Index	: 1.3328		Viscosity	: 0.8878	(cP)

Analysis Results

Zeta Potential	: -41.95	(mV)	Zeta Potential of Cell (Upper)	: -29.64	(mV)

Figure 31*(a2Zeta potential for AgNPsEaqSW

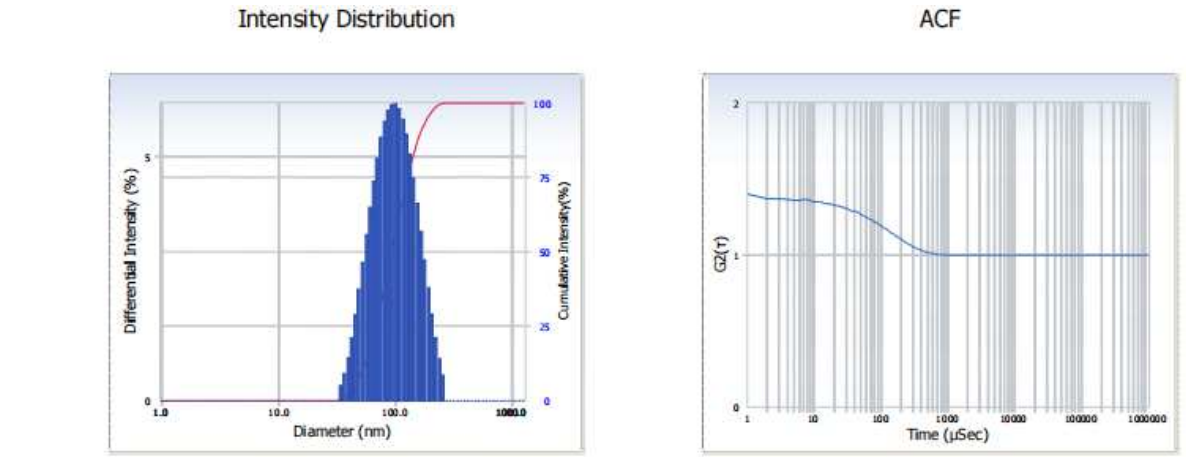

Distribution Results (Contin)

Peak	Diameter (nm)	Std. Dev.

Cumulants Results

Diameter (d) : 90.5 (nm)

Polydispersity Index (P.I.) : 0.158

Figure S31*(b1) Hydrodynamic diameter, polydispersity index for AgNPsEETOHSW

Version 3.73 / 2.30

Measurement Condition

Sampling Time	: 400	(µs)	Correlation Method	: TD	
Correlation Channel	: 512	(ch)	Accumulation times	: 10	(times)
Scattering Angle	: 15.0	(°)	Temperature	: 25.1	(°C)
Intensity	: 78454	(cps)	Attenuator 1	: 4.2	(%)
Cell Center	: X: 6.710	(mm)	Attenuator 2	: 5.510	(%)
	Z: 6.945	(mm)	Pinhole	: 50	(µm)
Cell Constant	: 187.620	(1/cm)			
Cell Type	: Flow Cell				
Apply Voltage Type	: NEGATIVE				

Electric Field

Avg. Electric Field	: -6.06	(V/cm)	Avg. Current	: -0.32	(mA)

Diluent Properties

Diluent Name	: WATER		Dielectric Constant	: 78.2	
Refractive Index	: 1.3328		Viscosity	: 0.8858	(cP)

Analysis Results

Zeta Potential	: -57.14	(mV)	Zeta Potential of Cell (Upper)	: -64.73	(mV)

Figure 31*(b2) Zeta potential for AgNPsEETOHSW

Face 24 Hydrodynamic diameter, polyspermity index and Zeta potential (mV) of green naoparticles in colloidal solution

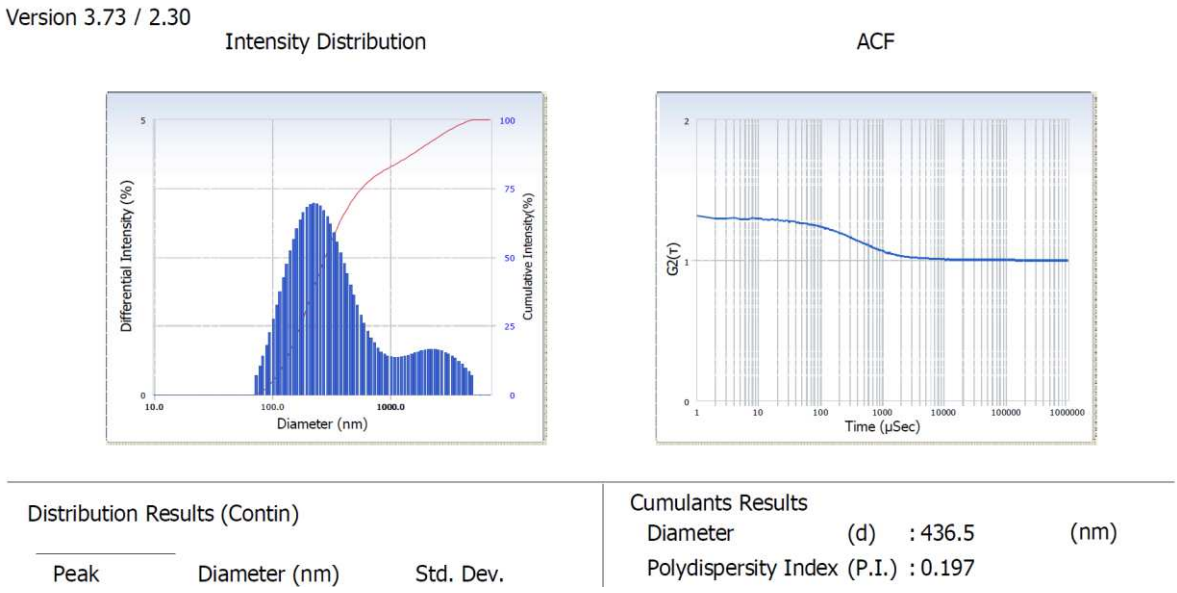

Figură 31 **(c1) Indicele de polidispersitate AuNPsEaqSW**

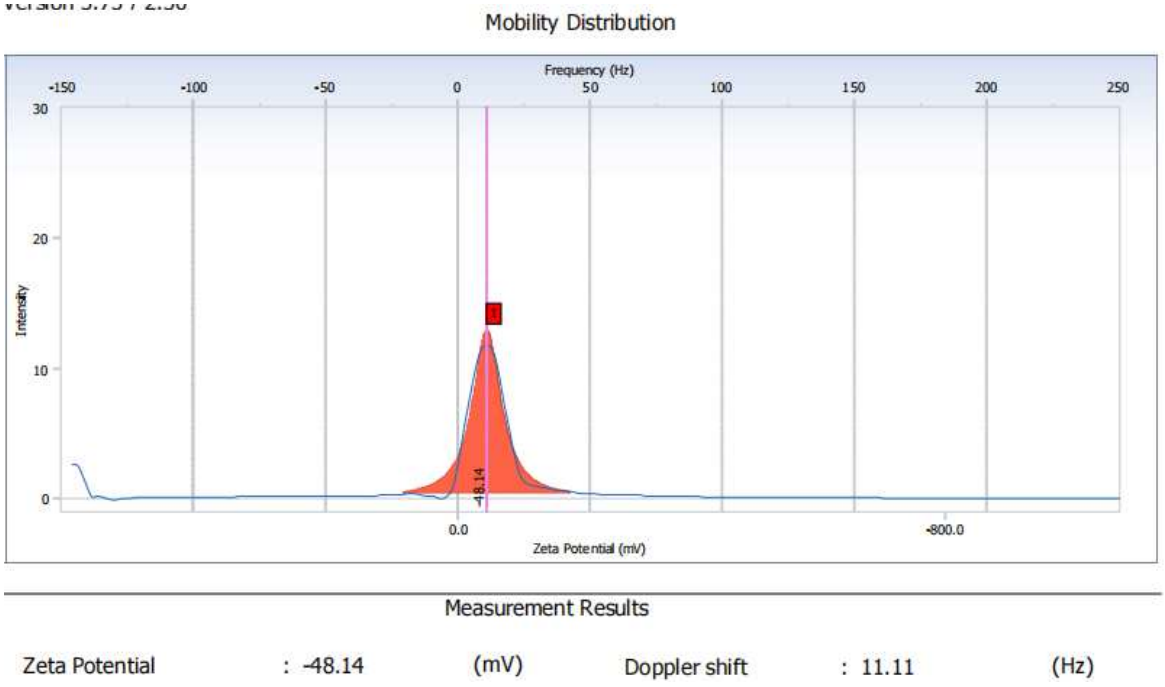

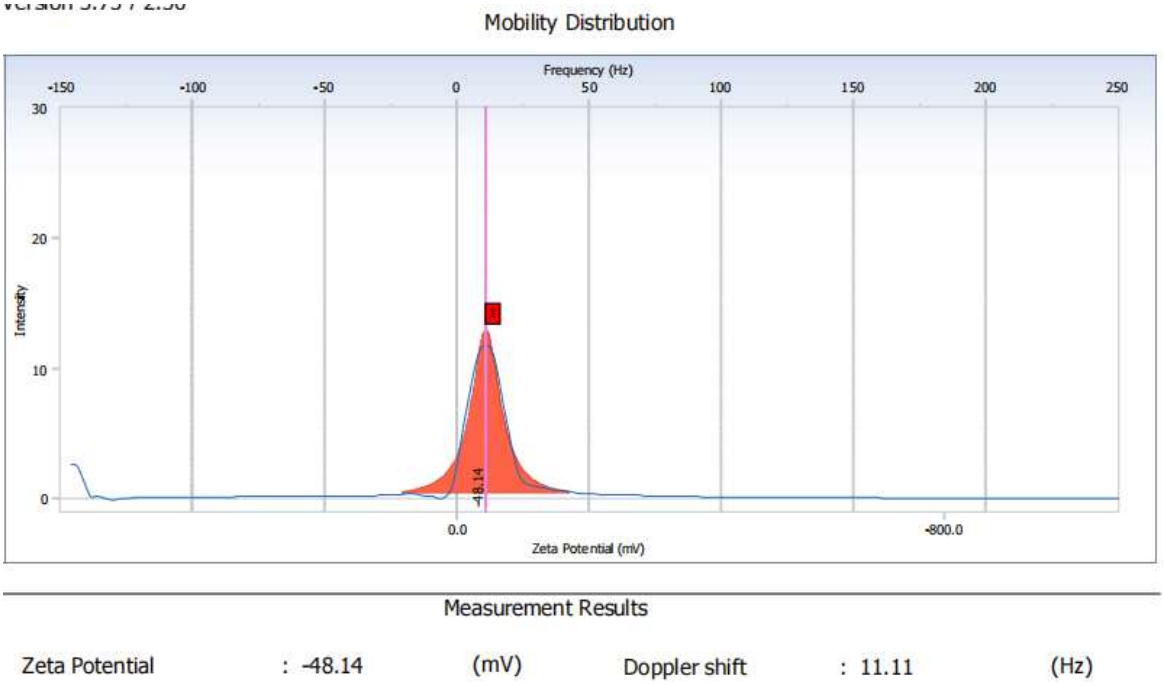

Figure 31* (c2) Zeta potential for AuNPsEaqSW

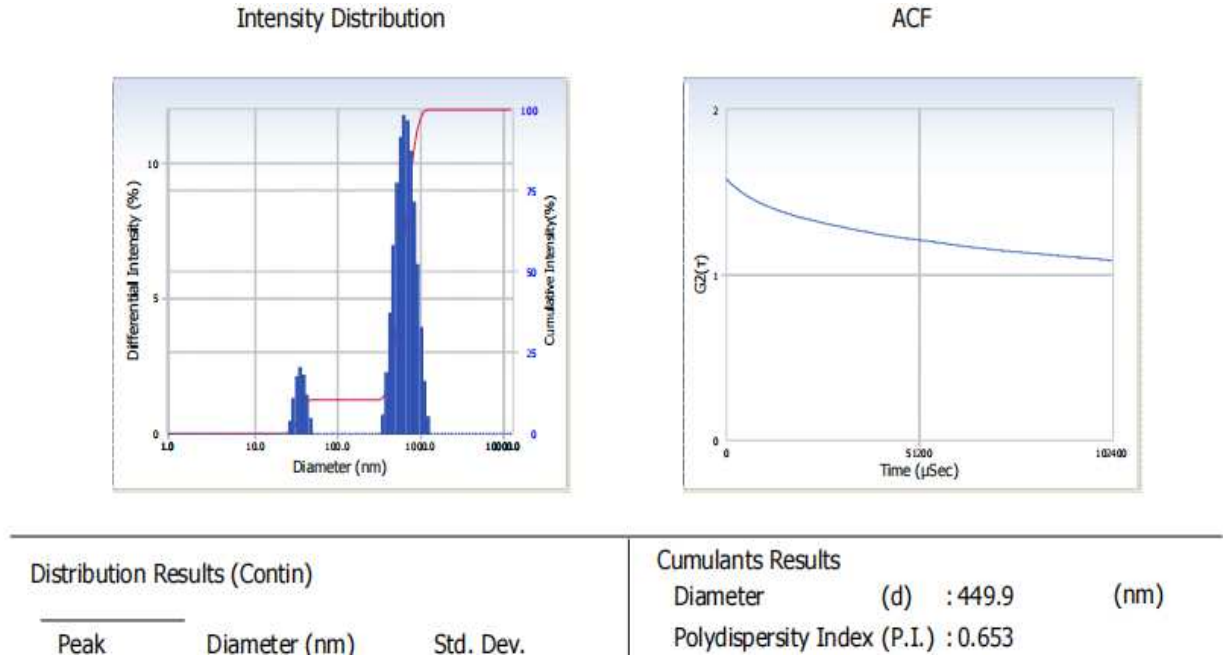

Figură 31 ***(d1) Hydrodinamic diameter, polydispersity index for AuNPsEETOHSW**

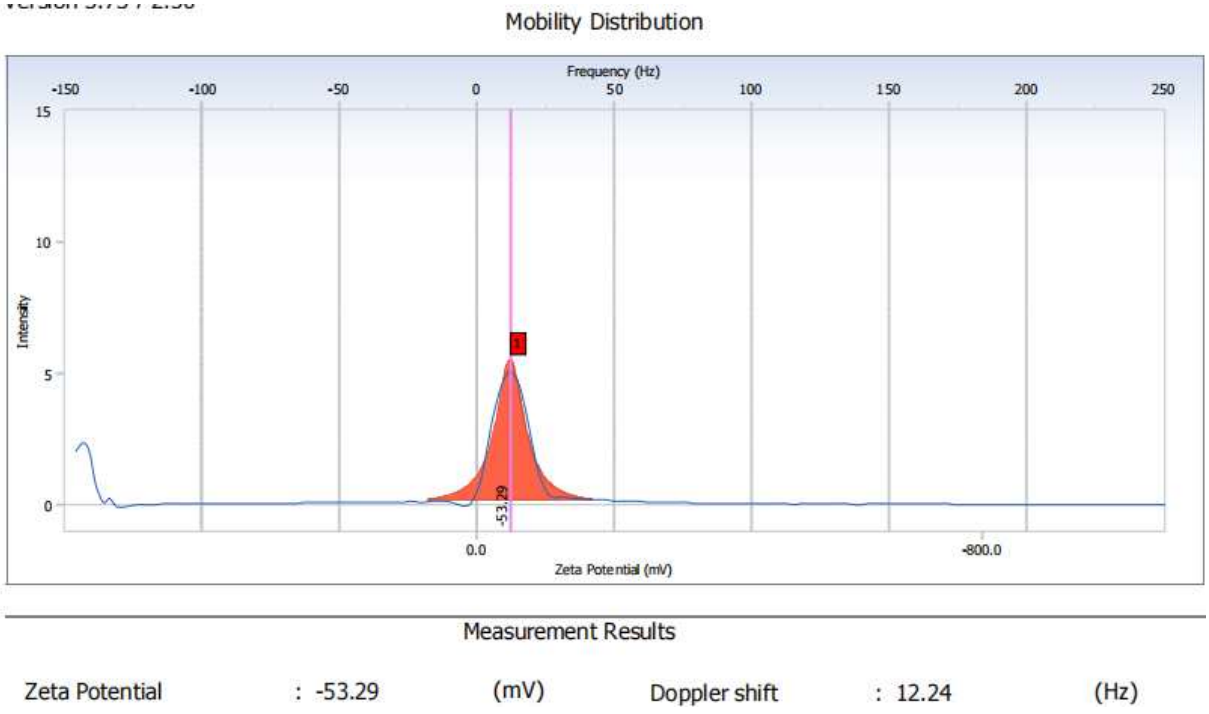

Figure 31 (d2) Zeta Potential for AuNPsEETOHSW

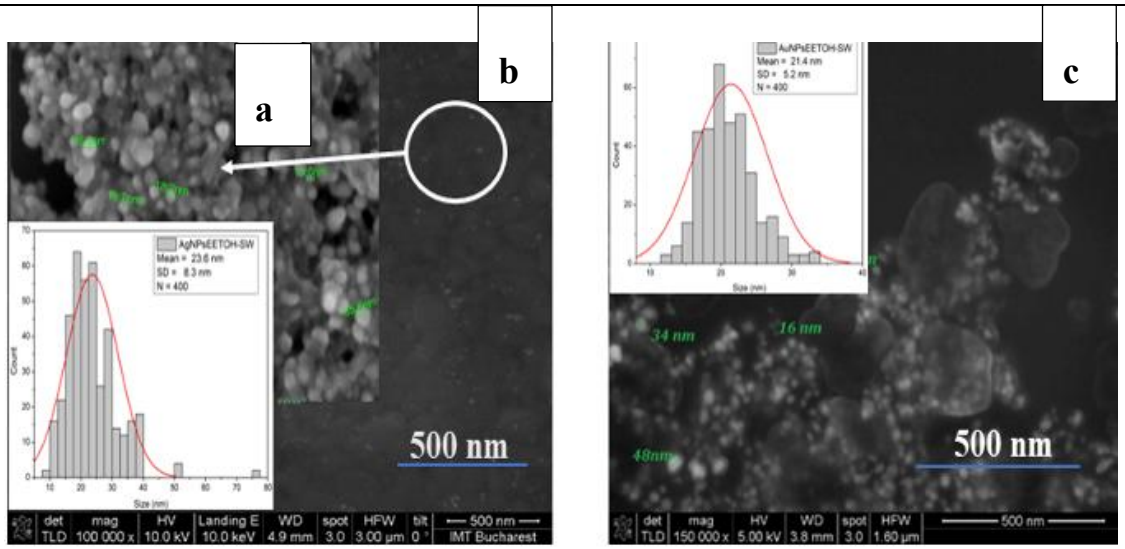

Face 25 SEM images at different sizes **a.** AgNPsEETOHSW (100 000x); **b.** AgNPsEETOHSW (300 000x); c. AuNPsEETOHSW (150 000x).

Figure 33 (a-d) shows TEM images for all samples analyzed.

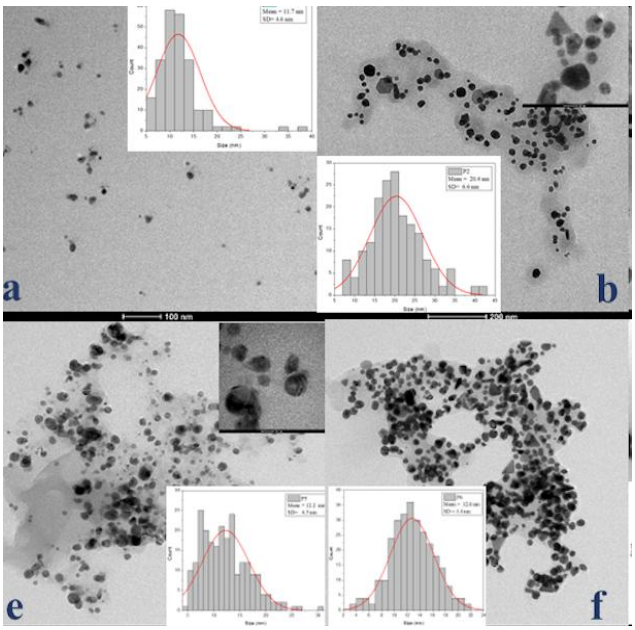

Face 26 - TEM images for all analyzed samples

From the TEM analysis of all samples, the Au and Ag nanoparticles predominantly showed a spherical morphology.

5.3.1.7.4. Dimensional and morphological characterisation of Melissa officinalis-based nanoparticles by DLS and PDI

The size distribution measured by DLS shown in Figure 34 showed two populations: particles with sizes between 75 nm – 255 nm, with a maximum at 143 nm; larger particles with a center at 1108 nm, probably attributed to plant extract remains.

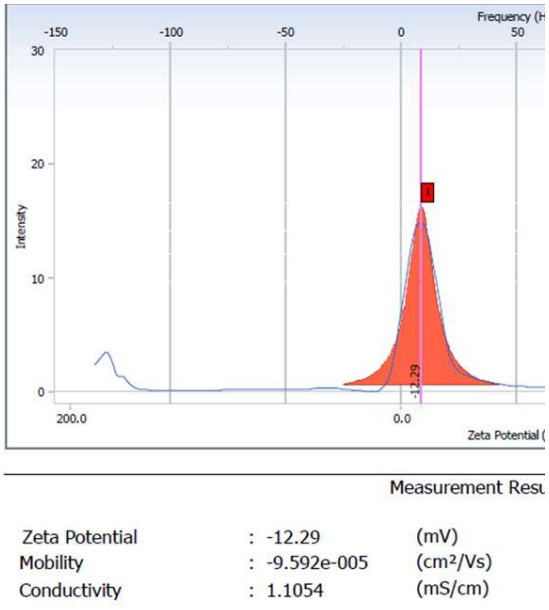

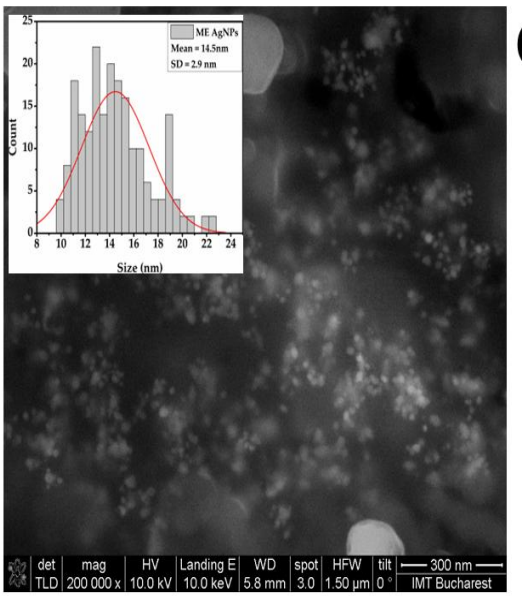

Face 27 (a)Change of the color of the solution from red-brown to dark brown as a result of Ag bioreduction by Melissa officinalis extract; - Figure 1(a)- DLS recorded for ME AgNPs; (b) UV-Vis Spectra UV-Vis Spectra of ME AgNPs samples obtained by time reduction with Melissa officinalis extract(c) UV-Vis spectrum of 0.5mM AgNO3 solution- Figure 1(b). Zeta potential for ME AgNPs

Scanning electron microscopy (SEM) presented confirmed that the real nanoparticles are much smaller than those observed by **Dynamic Light Scattering (DLS)** at, due to their coating with bioactive compounds in the extract. *Melissa officinalis* extract has been successfully used for the biosynthesis of silver nanoparticles, generating relatively stable nanoparticles with controllable size. ME AgNPs nanoparticles have demonstrated well-defined optical and structural characteristics, having a high potential for use in therapeutic and pharmacological applications.

5.3.2 Antimicrobial assessment

5.3.2.1 Evaluation of the antimicrobial activity of nanoparticles synthesized with Salix alba

SAgNPs-WT obtained by "green synthesis" from willow bark were tested against different dosage forms, with and without active substances, to highlight the possible positive and negative control effect, observing an antibacterial effect on all three bacteria tested. For *E.c* and *P.a*, the efficiency of the solutions increases with dilution (at 600 nm), while for *S.a*, the nanoparticle solutions seem to have only a small effect on the change in efficiency, which varies around 50%, but shows a low downward trend.

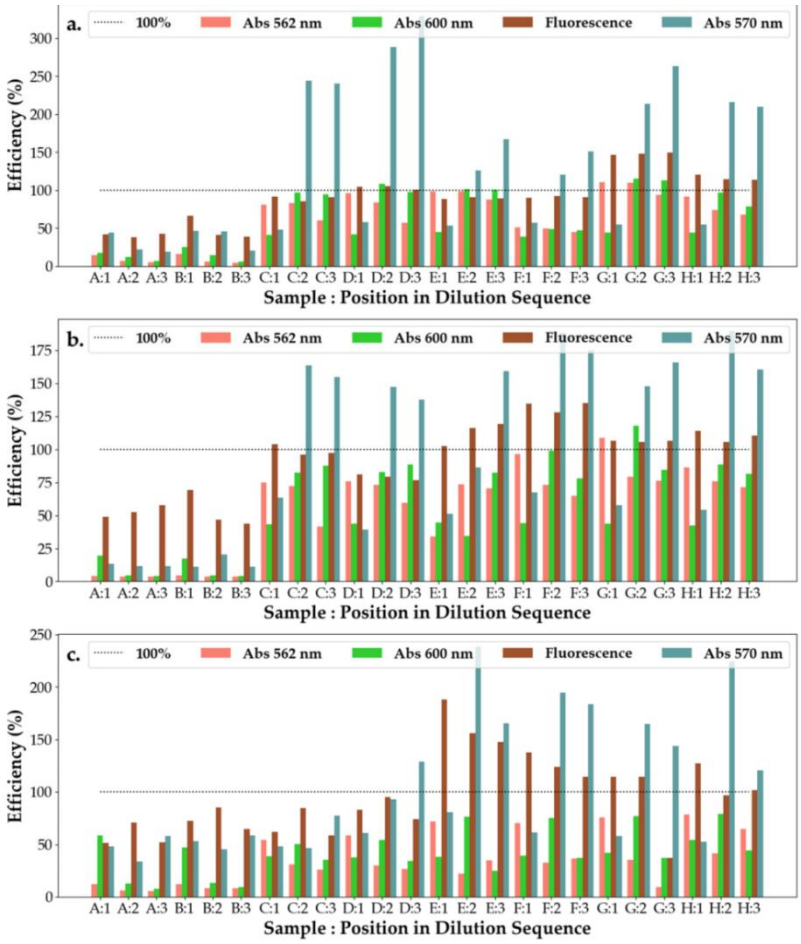

Face 28 Antibacterial response efficiency (η) of SAg/AuNP-WT samples at three dilution levels tested against (a) Escherichia coli, (b) Pseudomonas aeruginosa, and (c) Staphylococcus aureus. A–H samples are the following

solutions tested against bacteria: A—SAuNPs-WT 1S; B-SAgNPs-WT 1S; C—White Willow Extract; D—White Willow Extract; E—SAuNPs-WT 7S; F—SAuNPs-WT 10S; G—SAuNPs-WT 7S; and H-SAuNPs-WT 10S

The PCA components were mapped until one component accounted for less than 5 % of the data variation, with 2D representations of the characteristic space being shown in Figure 40A for the fluorescent and 570 nm measurements and in Figure 40b for the 562 nm and 600 nm measurements. In addition, the characteristic maps for the main components (PC) are shown in Figure 36 a,b.

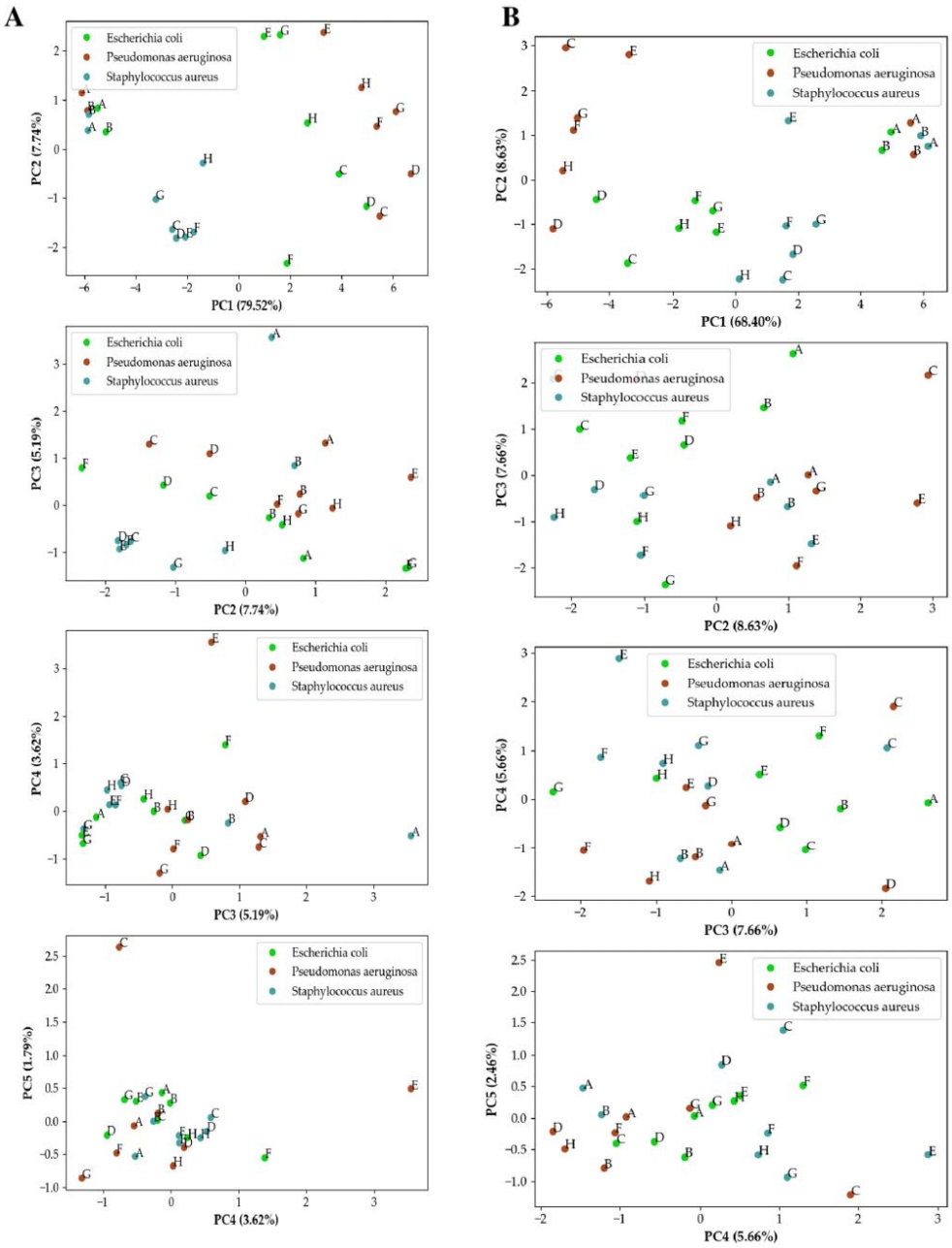

Face 29 PCA Representation for Single Wavelength Measurements for SAg/AuNPs-WT(a)

PCA Representation of Multi-Wavelength Measurements for SAg/AuNPs-WT (b)

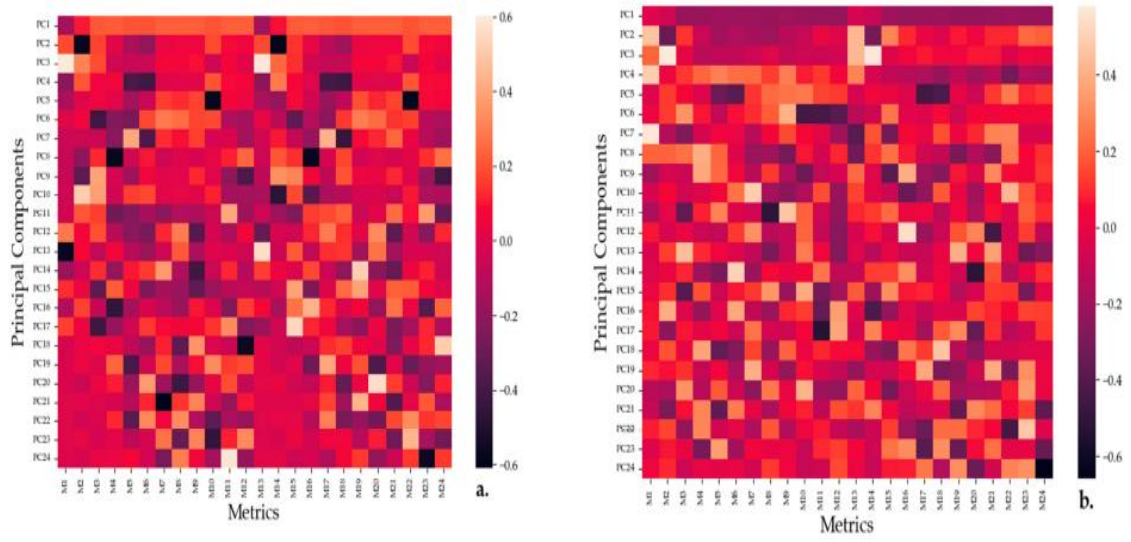

Face 30 Characteristics representing the correlation between the information explained by the approximate main components (PCs) by PCA and the characteristics collected during the analysis of the Ou/AgNP-WT samples

Characteristics show the correlation between PC and a particular feature, with darker colors signifying an inverse correlation and lighter colors signifying a direct correlation. The fact that samples A and B are the ineffective substances for measurements is further confirmed by PCA Figure 38, as all these measurements are grouped together, regardless of the bacterium being queried.

5.3.2.1.1 Evaluation of antimicrobial activity of Salix alba-based formulations (hydrogel)

It can be seen from Figure 42 a, b that solution H is the most receptive to a change in dilution, having the greatest variation from the mean, as shown by the first main component. However, this answer for H seems to come regardless of the interaction with a specific cell culture.

In addition, PC2 serves as a classifier for the response of the hydrogel solution to *S.a*, since at the third dilution, no hydrogel solution has significant efficiency when measured at 562 nm and 600 nm. PC3 also appears to differentiate the effects of the hydrogel on P.a, with responses being closer to white and negative white, both under 562 nm light and under 600 nm excitation for this interaction.

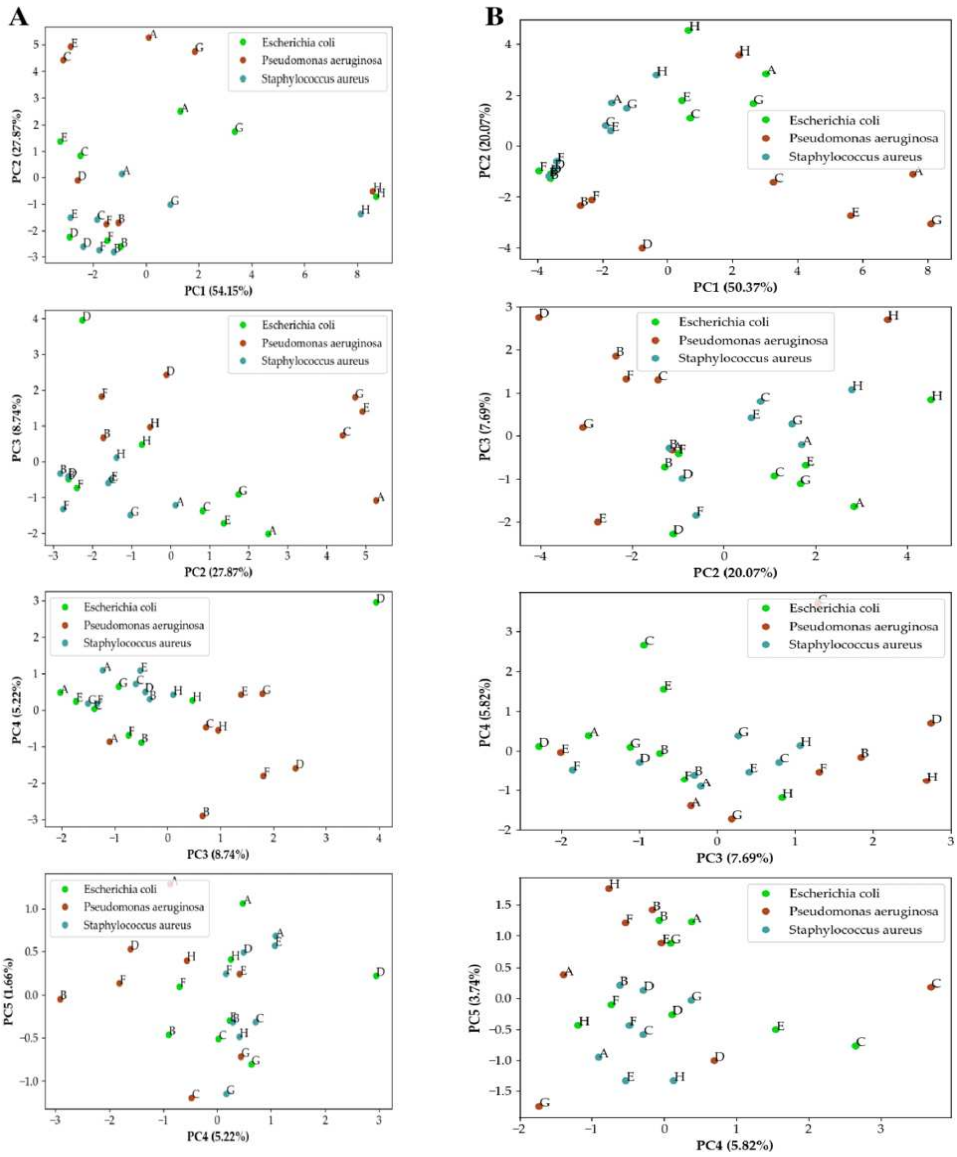

Face 31 PCA representation for single-wavelength measurements for hydrogels (a); PCA Representation of Multi-Wavelength Measurements for Hydrogels (b)

From Figure 39 it can be seen again that H does not seem to vary with cell culture; therefore, it could be used as a reference measurement for all other substances. PC2 correlates with a strong light response of 570 nm and thus can be used to differentiate the response to P.a from all other cell cultures.

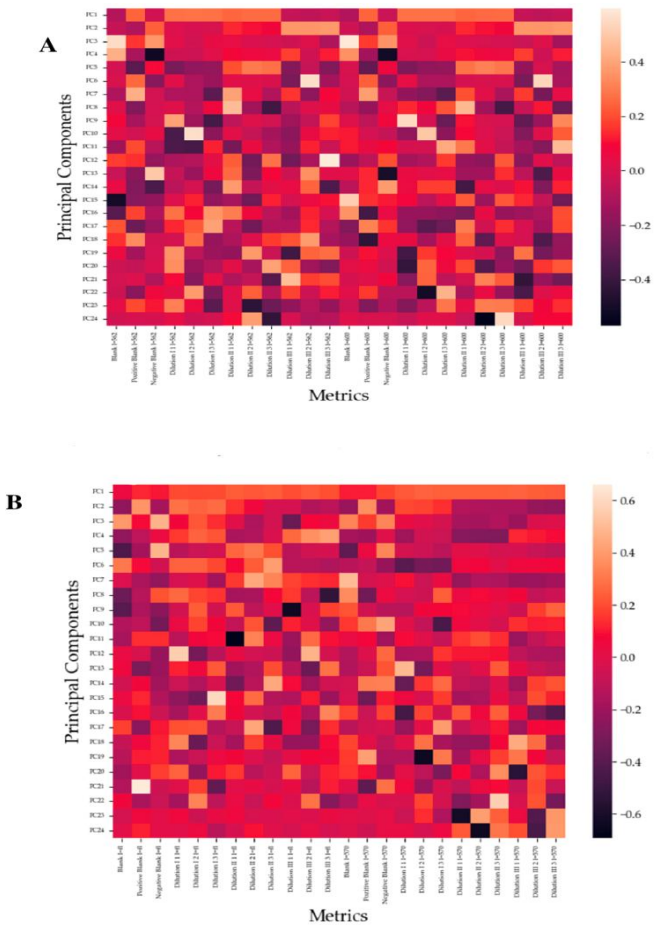

Face 32 Characteristics of single-wavelength measurements for hydrogels (a) multi-wavelength measurements for hydrogels (b)

In Figure 40 it can be seen that the efficiency of the ointment measured by excitation at 570 nm increases strongly with dilution of the substances when interacting with *P.a*, while there was no significant response to interaction with the other two cell cultures.

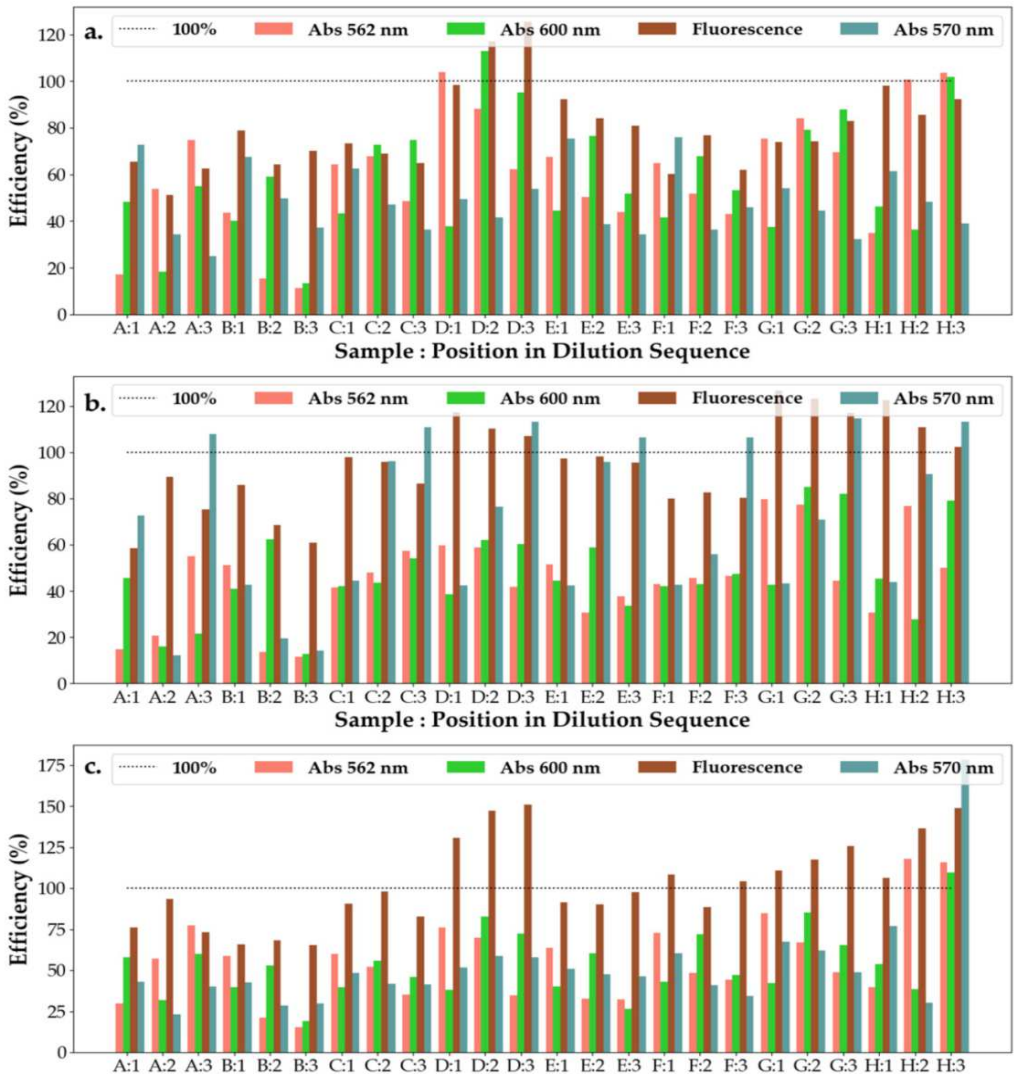

*Face 33 Antibacterial response (η) efficiency of SAgNPs-WT ointment samples at three dilution levels tested against (**a**) Escherichia coli, (**b**) Pseudomonas aeruginosa and (**c**) Staphylococcus aureus. Probele A-H reprezintă următoarele soluții testate împotriva bacteriilor: A-Tween 20; B-Ont 1 + SAgNPs-WT 10S + 1% tween 20; C-Ont 1 + SAgNPs-WT 10S + 1% tween 20 (1:1:1); D-Ont 1+SAgNPs-WT 10S+1% tween 80 (1:1:1); E-Ont 2 + SAgNPs-WT 10S + 1% tween 80; F-Ont 2 + SAgNPs-WT 10S + 1% tween 20 (1:1:1); G-Ont 2 + SAgNPs-WT 10S + 1% tween 80 (1:1:1); și H-Tween 80*

From the PCA measurement for the ointment shown in Figure 46 a,b there does not appear to be a group of all three cell cultures that is close enough to suggest a reference solution. However, under excitation of 562 nm and 600 nm, no ointment seems to be very selective. PC2, which differentiates between the third and first dilutions, seems to serve as a good indicator of the effectiveness of ointments against *P.a*, the only exception being B ointment.

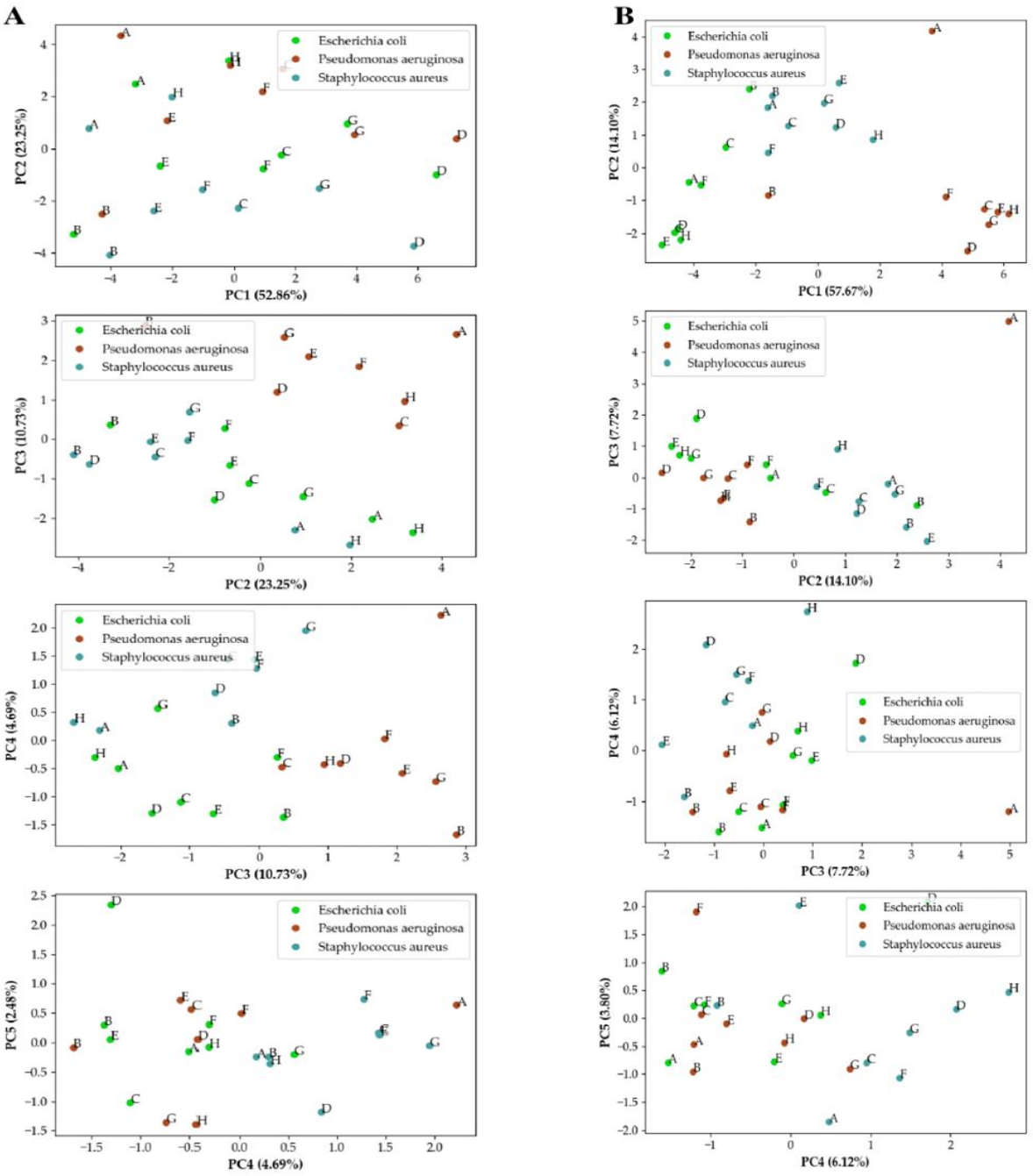

Face 34 PCA Representation for Single Wavelength Measurements for Ointments (a), Multi-Wavelength for Ointments (b)

For measurements at 570 nm and fluorescence Figure 42 PC1 shows a good split between the response to *P.a* and the other cell cultures due to the strong increase in efficiency with dilution when exposed to the excitation of 570 nm. The only exception is ointment B, which shows a decrease in efficiency under illumination to 570 nm with dilution.

Similarly, PC2, which shows the comparison between fluorescence and illumination at 570 nm, serves as a good classifier for the response to *S.a*, being characterized by consistently high differences between the two measurements in all dilutions.

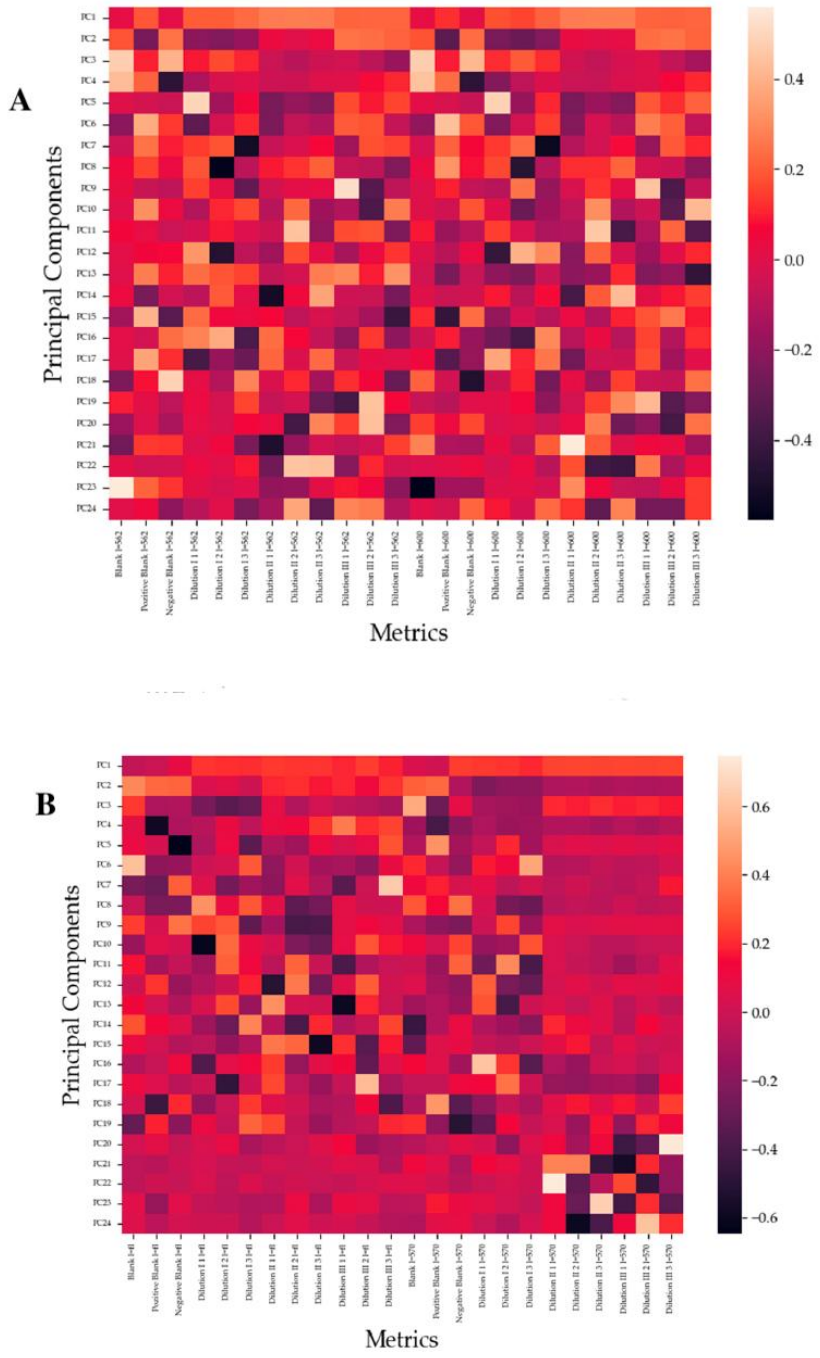

Face 35 Characteristic map for single-wavelength measurements for ointments (a); multi-wavelength for ointments (b)

5.3.2.2 EVALUATION OF THE ANTIMICROBIAL ACTIVITY OF NANOPARTICLES SYNTHESIZED WITH ARTEMISIA ANNUA

The antifungal effect was evaluated on *Saccharomyces cerevisiae, Candida albicans, Penicillium sp* and *Aspergillus sp*, by incubation on solid Sabouraud media for 3 days to 1 week at 23-26º C, measuring the inhibition zone as in the case of bacteria.

Figure 43 illustrates the inhibition zone as a function of the inhibition concentration calculated for the pelinite samples

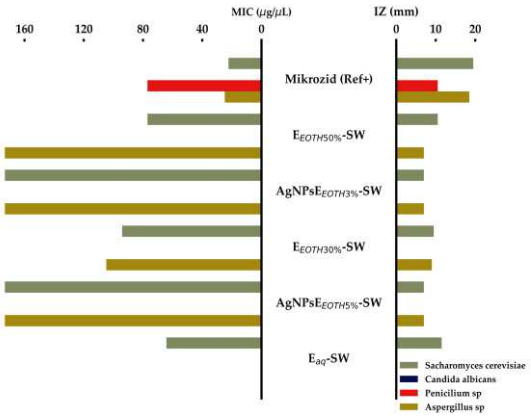

Face 37 Antifungal effect of aqueous/ethanolic extracts and nanoparticles obtained from Artemisia Annua

Legend: Mikrozid – 60% alcohol solution; EETOH50%-SW – 50% alcoholic extract of *Artemisia Annua*; EETOH30%-SW- 30% alcoholic extract from *Artemisia Annua*; AgNPsEETOH5%- SW- obtained by reducing silver with 50% extract EETOH50%-SW (1 :10, extract: AgNO3 1mM – v:v); AgNPsEETOH3%-SW- obtained by silver reduction EETOH30%-SW (1 :10, extract: AgNO3 1mM – v:v)

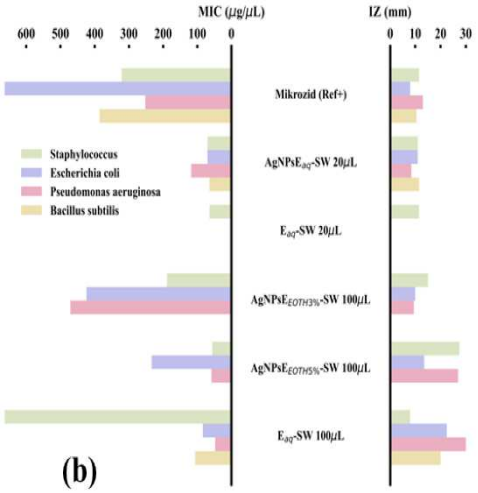

Face 36 Representation of the calculated inhibition zone for Artemisa annua

The antifungal effect of the nanoparticles was shown in Figure 44 for sweet wormwood samples.

5.3.3 IN VITRO ASSESSMENT OF CYTOTOXIC AND SYNERGISTIC EFFECT

5.3.3.1 IN VITRO EVALUATION OF THE CYTOTOXIC AND SYNERGISTIC EFFECT OF SALIX ALBA EXTRACT AND NANOPARTICLES

The cytotoxicity of SAgNPs-WT was assessed by MTT and LDH assays using HaCaT cell lines Figure 48 a,b. The inflammatory response was analyzed using the Griess method[250]. At 24 and 48 h, after exposure of keratinocytes to different concentrations of NPs (0.4-17.5 µg/mL), the nitric oxide production in the culture medium was tested, which is shown in Figure 45.

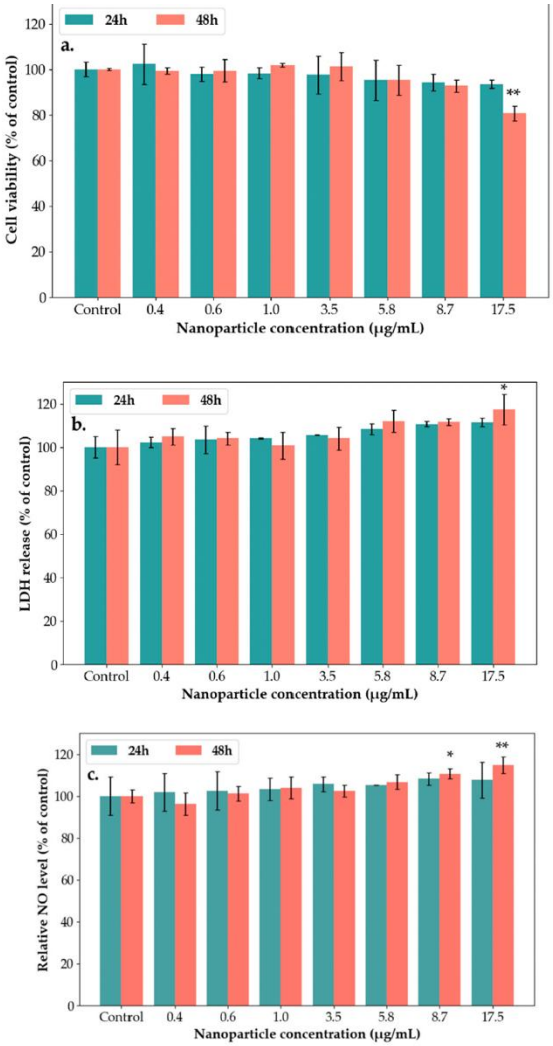

*Face 38 Biological tests performed on SAg/AuNPs-WT using the following techniques: (a) Test MTT after 24 h and 48 h of exposure to different concentrations of SAgNPs-WT in keratinocytes. Cell viability was normalized in untreated cells (without SAgNPs-WT). Results are expressed as mean ± SD (n = 3) and presented as percentage (%) of control. (b) Lactate dehydrogenase (LDH) activity released after 24 h and 48 h of exposure to different concentrations of SAgNPs-WT in HaCaT cells. Results are expressed as mean ± SD (n = 3) and reported as percentage (%) compared to control. (c) Effects of SAgNPs-WT on nitric oxide (NO) production in HaCaT cells. The cells were treated with SAgNPs-WT (0.4–17.5 µg/mL) for 24 h and 48 h. Results are expressed as mean ± SD (n = 3) and reported as percentage (%) compared to control. Statistical indications: p < 0.01 (significantly high), * p < 0.05 (significant moderate*

In Figure 45a, MTT results showed a decrease of approximately 20% after 48 h at concentrations of 17.5 μg/mL of NP compared to the control level. No significant changes were recorded for the other concentrations.

5.3.3.2 IN VITRO EVALUATION OF THE CYTOTOXIC AND SYNERGISTIC EFFECT OF ARTEMISIA ANNUA-BASED EXTRACT AND NANOPARTICLES

The studies were conducted in vitro to investigate the effect of the samples tested on human tumor cells LoVo (human colon adenocarcinoma) and MDA-MB-231 (human breast adenocarcinoma) and on the hepatic tumor line HepG2 compared to the normal HUVEC cell line (human umbilical vein endothelial cells).

The positive controls of the study were CisPt and DOX, which are commonly used to treat colon and breast cancer, respectively. To assess cell viability, dilutions of the initial colloidal solutions were performed and the cell lines were exposed for 24 and 48 hours. CisPt and DOX appear to affect the investigated tumor lines; however, their effects also extended to the normal cell line after 24 hours (Figure 46(a)).

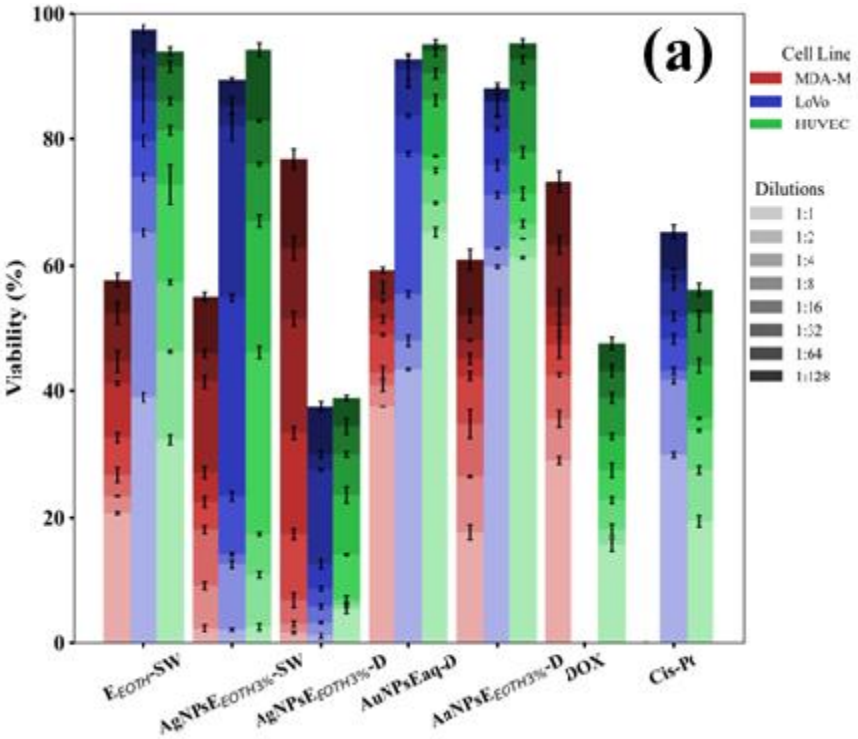

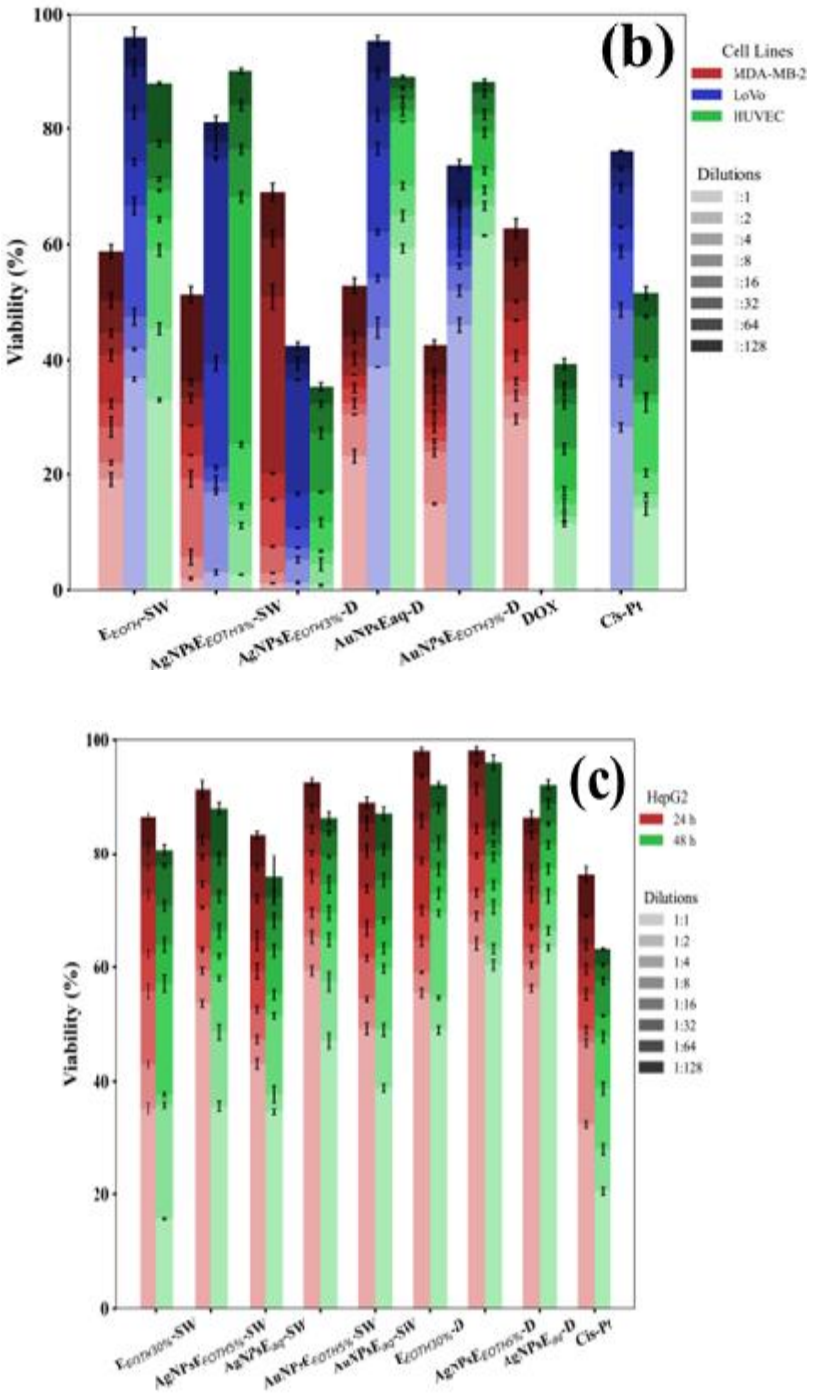

Face 39 Effect of different dilutions of dandelion and pelinite-based sample on viability (%) of human cancer cell lines: breast cancer (MDA-MB-231), human colorectal adenocarcinoma cell line LoVo, and endothelial cells in human umbilical vein HUVEC at (a) 24h and (b) 48h; (Dilutions are given by the hue of the stacked bar graphs, with a lighter hue corresponding to a lower dilution); (c) Effect of different dilutions of the dandelion and dandelion-based sample on the viability (%) of HepG2 (human liver carcinoma cell line) at 24h and 48h. Dilutions are given by the hue of the stacked bar graphs, with a lighter hue corresponding to a lower dilution.

5.3.3.3 IN VITRO EVALUATION OF THE CYTOTOXIC AND SYNERGISTIC EFFECT OF LEMON BALM EXTRACT AND NANOPARTICLES

The combination of alcohol extract and biogenic silver nanoparticles (ME AgNPs) can improve the effectiveness of the treatment and could be just as effective, or even more effective, with minimal toxic effects on normal cells. Thus, the cytotoxic effect of extracts derived from Melissa officinalis was evaluated 24 and 48 hours after treatment. Figures 47(a) and 25(b) show measurements of cell viability at 24 and 48 hours of extract treatment, respectively, compared to drugs administered individually.

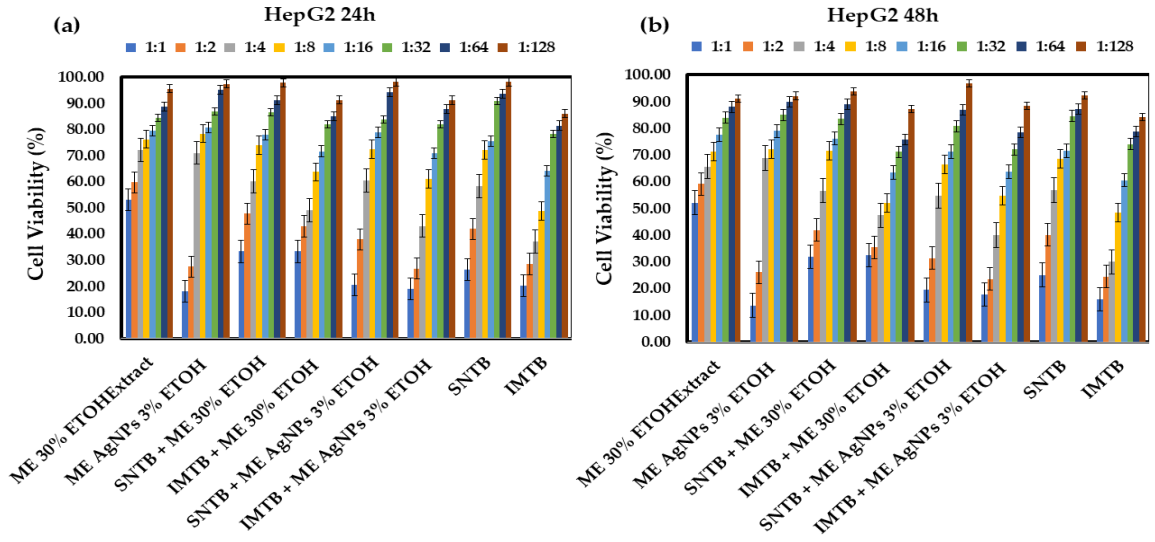

Face 40 Cell viability (%) of HepG2 lines after: (a) 24 hours of treatment with different dilutions of samples based on *Melissae extractum* and the chemotherapy drugs Sunitinib and Imatinib, and (b) show the same measurements after 48 hours of treatment

5.4 CONCLUSIONS

Regarding the physicochemical characterization of nanoparticles, silver and gold nanoparticles have been successfully obtained by bioreduction of plant extracts (*Salix alba, Artemisia annua, Melissa officinalis*). UV-Vis spectroscopy, FTIR, PL, XRD and electron microscopy (SEM/TEM) confirmed the formation of the nanoparticles and their composition.

SAgNPs-WTs have demonstrated long-term stability and stable behavior in environments with varying pH. The size and shape of the particles were correlated with the synthesis parameters and the extract used, and the nanoparticles were mostly spherical, with dimensional distributions between 10–76 nm. The antimicrobial evaluation showed that SAgNPs-WT had a significant antibacterial effect, especially on Pseudomonas aeruginosa and Staphylococcus aureus.

Formulations such as hydrogels and ointments improved antimicrobial activity, particularly when combined with dispersing agents (Tween 20). Comparatively, nanoparticles

derived from *Artemisia annua* showed less antibacterial activity and limited antifungal effect, possibly due to the more complex structure of the fungal cell wall.

In vitro evaluation of the cytotoxic and synergetic effect showed that SAgNPs-WT exhibited reduced keratinocyte cytotoxicity (HaCaT) up to a certain concentration, indicating a safe potential for pharmaceutical applications. Extracts and nanoparticles from *Artemisia annua* and *Melissa officinalis* showed selective cytotoxic effects on tumor lines, especially MDA-MB-231 (breast), LoVo (colon) and HepG2 (liver).

The synergistic effect of nanoparticles with chemotherapy drugs resulted in increased antitumor efficiency and low toxicity on normal cells, indicating a high therapeutic potential. In conclusion, the biosynthesis of nanoparticles from plant extracts is an ecological, efficient and promising method for obtaining functional nanomaterials.

SAgNPs-WT is distinguished by increased stability, significant antimicrobial activity and biocompatibility, representing an ideal candidate for the development of topical pharmaceuticals (gels, ointments).

Artemisia *and* Melissa *extracts*, in combination with nanoparticles, have potential in oncological treatments, due to their synergistic effect and selective cytotoxicity on tumor cells. The size, morphology, and surface composition of nanoparticles are essential for their bioactive properties, and full characterization is crucial for medical applications.

Overall, the results support the use of biosynthesized nanoparticles in biomedical applications, providing a safe and effective alternative to conventional treatments.

The results of this chapter were published in the following articles:

1. Mirela Claudia Rimbu, Liliana Popescu, Mirela Mihăilă, Roxana Colette Sandulovici, **Daniel Cord***-autor corespondent, Carmen Marinela Mihailescu, Mona Luciana Galatanu, Mariana Panturoiu, Carmen Elisabeta Manea, Adina Boldeiu, Oana Brincoveanu, Mihaela Savin, Alexandru Grigoroiu, Florin Dan Ungureanu, Emilia Amzoiu, Mariana Popescu, Elena Truta, *Synergistic Effects of Green Nanoparticles on Antitumor Drug Efficacy in Hepatocellular Cancer*, Biomedicines 2025, 13, 641, https://doi.org/10.3390/biomedicines13030641 , **FI=3,9**
2. Mirela Claudia Rimbu, **Daniel Cord***-autor corespondent, Mihaela Savin, Alexandru Grigoroiu, Mirela Antonela Mihăilă, Mona Luciana Gălățanu, Viorel Ordeanu, Mariana Panțuroiu, Vasilica Țucureanu, Iuliana Mihalache, Oana Brîncoveanu, Adina Boldeiu, Veronica Anăstăsoaie, Carmen Elisabeta Manea, Roxana Colette Sandulovici, Marinela Chirilă, Adina Turcu Știololică, Emilia Amzoiu, Victor Eduard Peteu, Cristiana Tănase, Bogdan Firtat, Carmen Marinela Mihăilescu, *Harnessing Plant-Based Nanoparticles for Targeted Therapy: A Green Approach to Cancer and Bacterial Infections*, *Int. J. Mol. Sci.* **2025**, *26*(14), 7022; https://doi.org/10.3390/ijms26147022 , **FI=4,9**
3. **Daniel Cord**, Mirela Claudia Rimbu, Cristiana Tănase, Cristina Tăbleț, Gheorghe Duca, *Molecular docking study of some active principles from Silybum marianum, Chelidonium majus, Ginkgo biloba, Gelsemim sempervirens, Artemisia annua and Taraxacum officinale*, Chemistry Journal of Moldova. General, Industrial and Ecological Chemistry. 2025, 20(1), 100-105 https://doi.org/10.19261/cjm.2025.1337 , **FI=0,5**
4. Mirela Claudia Rimbu, Dan Florin Ungureanu, Cosmin Modovan, Madalina Toba, Marinela Chirila, Elena Truta, **Daniel Cord**, *Cystic Hepatic GIST: A Case Report of Rare Presentation and Long-Term Survival,* Curr. Oncol. 2025, 32, 383 https://doi.org/10.3390/curroncol32070383 , **FI=3,4**

6. GENERAL CONCLUSIONS

This paper analyzed the antimicrobial properties of plant extracts of. Taraxacum officinale, Chelidonium majus, and Silybum marianum, as well as aloolic extracts from Artemisia annua.

Qualitative tests have shown that all plant extracts inhibited the growth and development of microbial tumines. Silybum marianum extract showed the strongest antimicrobial effect on gram-positive strains. The alcoholic extracts of Artemisia annua had a broad microbial spectrum, being effective against all strains except Staphylococcus aureus.

Quantitative determinations established the concentrations required for bacteriostatic and bactericidal effects. The microbial strains showed a higher sensitivity to tinctures compared to the alcoholic extracts of Artemisia annua.

In *vitro studies* have also highlighted the antibiofilm activity of the extracts. *Chelidonium majus*, *Silybum marianum* and *Artemisia annua* inhibited biofilm formation in all tested strains. Taraxacum officinale tincture was especially effective against gram-negative bacteria and fungi.

The results obtained are promising and support the need for further studies on the biochemical composition of these extracts. Future research could facilitate the development of effective strategies against bacterial and fungal infections.

Another object of the study was the development and characterization of nanoparticles obtained by green synthesis using Artemisia annua extract. These have been tested in topical pharmaceutical formulations.

Gold nanoparticles showed antimicrobial activity, but their tendency to flocculate made them less suitable for pharmaceutical formulations. All nanoformulations tested, which contained silver nanoparticles, demonstrated high potential as antimicrobial and anti-inflammatory agents.

Cells exposed to silver nanoparticles showed no signs of cytotoxicity at the concentrations used for antimicrobial tests. These compounds could be integrated into anti-infective drugs, hygiene products and cosmetics for the treatment of injuries caused by various pathologies.

Silver nanoparticles obtained by green synthesis from Salix alba bioextracts have demonstrated antimicrobial and antibiofilm activity. Hydrogels formulated with these nanoparticles showed high physicochemical stability and increased antibacterial activity, being more effective than gold nanoparticles.

This paper also has a number of limitations. The studies were conducted only in vitro. The effects in the living organism may be different due to bioavailability, metabolism or immune response. Plant extracts can have variable chemical compositions depending on the season, geographical area, extraction method, which affects reproducibility. Antimicrobial testing was

performed on a small number of reference bacterial strains, without clinical or antibiotic-resistant strains.

The promising results of these extracts support further research to optimize formulations and test their stability and safety. To this end, further studies will be carried out regarding the validation of the efficacy of the formulation -tablets-, and the patenting process will be initiated.

This research opens up new perspectives for the use of natural compounds in innovative therapies, offering alternatives to conventional treatments.

The present study demonstrated the high potential of some native medicinal plants in the generation of bioactive compounds with antioxidant, antimicrobial and antitumor activity, as well as the applicability of their extracts in the biosynthesis of functional metal nanoparticles. The results obtained highlight important contributions in the field of green biotechnology, with direct implications in the development of new therapies and pharmaceutical products.

The evaluation of the antioxidant capacity of plant extracts indicated significant differences between the species analyzed, with *Artemisia annua* and *Taraxacum officinale* showing the highest free radical scavenging activity. This property is correlated with the high content of polyphenols and flavonoids, which can help prevent or relieve some conditions associated with oxidative stress. Despite a lower antioxidant capacity, plants such as *Silybum marianum* and *Chelidonium majus* are therapeutically valuable, having documented hepatoprotective and anti-inflammatory effects.

From an antimicrobial point of view, the plant extracts tested demonstrated variable bacteriostatic and bactericidal activity depending on the species and extraction solvent. *S. marianum* proved effective against Gram-positive strains, while *A. annua* showed a broad spectrum of antimicrobial action. In addition, the ability of certain extracts to inhibit the formation of bacterial biofilms was found, which is relevant for the control of persistent infections.

One of the central points of the work was represented by the biosynthesis of metallic nanoparticles (Ag and Au) using extracts of *Salix alba, Artemisia annua and Melissa officinalis*. The physicochemical characterization of these nanoparticles confirmed the formation of spherical and stable structures, ranging in size from 10 to 76 nm. SAgNPs-WTs have been distinguished by colloidal stability, antioxidant potential and superior antimicrobial activity, being validated as promising ingredients in topical formulations such as hydrogels and ointments.

In vitro biological evaluation showed that silver nanoparticles have low toxicity to human keratinocytes, suggesting a favorable safety profile for dermatological applications. Moreover, the combination of plant extracts with metal nanoparticles produced significant antitumor effects on cancer cell lines (breast, colon, liver), in some cases exceeding the effectiveness of common chemotherapy drugs. These results highlight a promising synergistic effect that could be exploited in alternative oncology therapies with low toxicity on healthy cells.

In conclusion, the paper strongly supports the applicability of green biosynthesis in obtaining functional nanomaterials with high therapeutic value. The integration of plant extracts into nanoparticle synthesis processes opens up innovative perspectives for the development of pharmacological and cosmetic products with a positive impact on human health and a sustainable ecological profile. Further research in this direction could lead to the identification of effective natural solutions against antimicrobial resistance and the optimization of personalized treatments in oncology.

7. SELECTED BIBLIOGRAPHY

206. Miethke, M., Pieroni, M., Weber, T., Brönstrup, M., Hammann, P., Halby, L., ... & Müller, R. (2021). Towards the sustainable discovery and development of new antibiotics. *Nature Reviews Chemistry*, *5*(10), 726-749.
207. Stewart-Wade, S. M., Neumann, S., Collins, L. L., & Boland, G. J. (2002). The biology of Canadian weeds. 117. Taraxacum officinale GH Weber ex Wiggers. *Canadian journal of plant science*, *82*(4), 825-853.
208. Gilca, M., Gaman, L., Panait, E., Stoian, I., & Atanasiu, V. (2010). Chelidonium majus–an integrative review: traditional knowledge versus modern findings. *Forschende komplementärmedizin/Research in complementary medicine*, *17*(5), 241-248.
209. Zielińska, S., Jezierska-Domaradzka, A., Wójciak-Kosior, M., Sowa, I., Junka, A., & Matkowski, A. M. (2018). Greater celandine's ups and Downs− 21 centuries of medicinal uses of chelidonium majus from the viewpoint of today's Pharmacology. *Frontiers in pharmacology*, *9*, 299.
210. Gracz-Bernaciak J., Mazur O., Nawrot R., 2021. Functional Studies of Plant Latex as a Rich Source of Bioactive Compounds: Focus on Proteins and Alkaloids. *Int. J. Mol. Sci*. 22(22), 12427.
211. Bahmani, M., Shirzad, H., Rafieian, S., & Rafieian-Kopaei, M. (2015). Silybum marianum: beyond hepatoprotection. *Journal of evidence-based complementary & alternative medicine*, *20*(4), 292-301.
212. Valková, V., Ďúranová, H., Bilčíková, J., & Habán, M. (2020). Milk thistle (Silybum marianum): a valuable medicinal plant with several therapeutic purposes. *The Journal of Microbiology, Biotechnology and Food Sciences*, *9*(4), 836.
213. Shahrajabian, M. H., Wenli, S. U. N., & Cheng, Q. (2020). Exploring Artemisia annua L., artemisinin and its derivatives, from traditional Chinese wonder medicinal science. *Notulae Botanicae Horti Agrobotanici Cluj-Napoca*, *48*(4), 1719-1741.
214. Ekiert, H., Świątkowska, J., Klin, P., Rzepiela, A., & Szopa, A. (2021). Artemisia annua–importance in traditional medicine and current state of knowledge on the chemistry, biological activity and possible applications. *Planta Medica*, *87*(08), 584-599.
218. Móricz, Á. M., Fornal, E., Jesionek, W., Majer-Dziedzic, B., & Choma, I. M. (2015). Effect-directed isolation and identification of antibacterial Chelidonium majus L. alkaloids. *Chromatographia*, *78*, 707-716
219. Jyoti, B. S. (2013). Chelidonium majus L.-a review on pharmacological activities and clinical effects. *Global Journal of Research on Medicinal Plants & Indigenous Medicine*, *2*(4), 238.
220. Wianowska, D., & Wiśniewski, M. (2015). Simplified procedure of silymarin extraction from Silybum marianum L. Gaertner. *Journal of chromatographic science*, *53*(2), 366-372.
221. Bijak, M. (2017). Silybin, a major bioactive component of milk thistle (Silybum marianum L. Gaernt.)—Chemistry, bioavailability, and metabolism. *Molecules*, *22*(11), 1942.
222. Roleira, F. M., Varela, C. L., Costa, S. C., & Tavares-da-Silva, E. J. (2018). Phenolic derivatives from medicinal herbs and plant extracts: anticancer effects and synthetic approaches to modulate biological activity. *Studies in Natural Products Chemistry*, *57*, 115-156.
223. Golbarg, H., & Mehdipour Moghaddam, M. J. (2021). Antibacterial Potency of Medicinal Plants including Artemisia annua and Oxalis corniculata against Multi-Drug Resistance E. coil. *BioMed research international*, *2021*(1), 9981915.
224. Marinas, I. C., Oprea, E., Chifiriuc, M. C., Badea, I. A., Buleandra, M., & Lazar, V. (2015). Chemical composition and antipathogenic activity of Artemisia annua essential oil from Romania. *Chemistry & biodiversity*, *12*(10), 1554-1564.
225. Donato, R., Santomauro, F., Bilia, A. R., Flamini, G., & Sacco, C. (2015). Antibacterial activity of Tuscan Artemisia annua essential oil and its major components against some foodborne pathogens. *LWT-Food Science and Technology*, *64*(2), 1251-1254
240. Dehelean, C. A., Marcovici, I., Soica, C., Mioc, M., Coricovac, D., Iurciuc, S., ... & Pinzaru, I. (2021). Plant-derived anticancer compounds as new perspectives in drug discovery and alternative therapy. *Molecules*, *26*(4), 1109.
241. Sammar, M., Abu-Farich, B., Rayan, I., Falah, M., & Rayan, A. (2019). Correlation between cytotoxicity in cancer cells and free radical-scavenging activity: In vitro evaluation of 57 medicinal and edible plant extracts. *Oncology Letters*, *18*(6), 6563-6571.

LIST OF PUBLICATIONS AND DISSEMINATION OF RESULTS

Papers published in extenso as first author in ISI-listed journals, indexed Web of Science:

1. Mirela Claudia Rimbu, Liliana Popescu, Mirela Mihăilă, Roxana Colette Sandulovici, **Daniel Cord***-autor corespondent, Carmen Marinela Mihailescu, Mona Luciana Galatanu, Mariana Panturoiu, Carmen Elisabeta Manea, Adina Boldeiu, Oana Brincoveanu, Mihaela Savin, Alexandru Grigoroiu, Florin Dan Ungureanu, Emilia Amzoiu, Mariana Popescu, Elena Truta, *Synergistic Effects of Green Nanoparticles on Antitumor Drug Efficacy in Hepatocellular Cancer*, Biomedicines 2025, 13, 641, https://doi.org/10.3390/biomedicines13030641 , **FI=3,9**
2. Mirela Claudia Rimbu, **Daniel Cord***-autor corespondent, Mihaela Savin, Alexandru Grigoroiu, Mirela Antonela Mihăilă, Mona Luciana Gălățanu, Viorel Ordeanu, Mariana Panțuroiu, Vasilica Țucureanu, Iuliana Mihalache, Oana Brîncoveanu, Adina Boldeiu, Veronica Anăstăsoaie, Carmen Elisabeta Manea, Roxana Colette Sandulovici, Marinela Chirilă, Adina Turcu Știololică, Emilia Amzoiu, Victor Eduard Peteu, Cristiana Tănase, Bogdan Firtat, Carmen Marinela Mihăilescu, *Harnessing Plant-Based Nanoparticles for Targeted Therapy: A Green Approach to Cancer and Bacterial Infections*, *Int. J. Mol. Sci.* **2025**, *26*(14), 7022; https://doi.org/10.3390/ijms26147022 , **FI=4,9**
3. **Daniel Cord**, Mirela Claudia Rimbu, Cristiana Tănase, Cristina Tăbleț, Gheorghe Duca, *Molecular docking study of some active principles from Silybum marianum, Chelidonium majus, Ginkgo biloba, Gelsemim sempervirens, Artemisia annua and Taraxacum officinale*, Chemistry Journal of Moldova. General, Industrial and Ecological Chemistry. 2025, 20(1), 100-105 https://doi.org/10.19261/cjm.2025.1337 , **FI=0,5**
4. Mirela Claudia Rimbu, Dan Florin Ungureanu, Cosmin Modovan, Madalina Toba, Marinela Chirila, Elena Truta, **Daniel Cord**, *Cystic Hepatic GIST: A Case Report of Rare Presentation and Long-Term Survival,* Curr. Oncol. 2025, 32, 383 https://doi.org/10.3390/curroncol32070383 , **FI=3,4**

Papers published in extenso as first author in PubMed indexed journals:

5. **Daniel Cord**, Mirela Claudia Rimbu, Liliana Popescu, *New prospects in oncotherapy: bioactive compounds from Taraxacum officinale*, Medicine and Pharmacy Reports, https://doi.org/10.15386/mpr-2875

Works published in extenso, as co-author

6. Sandulovici, Roxana Colette, Mihailescu Carmen-Marinela, Alexandru Grigoroiu, Carmen Aura Moldovan, Mihaela Savin, Viorel Ordeanu, Sorina Nicoleta Voicu, **Daniel Cord,** Gabriela Mariana Costache, Mona Luciana Galatanu, and et al. 2023. "The Physicochemical and Antimicrobial Properties of Silver/Gold Nanoparticles Obtained by “Green Synthesis” from Willow Bark and Their Formulations as Potential Innovative Pharmaceutical Substances" *Pharmaceuticals* 16, no. 1: 48. https://doi.org/10.3390/ph16010048 **FI-=4,3**

Papers presented at national and international scientific events:

7. **Daniel Cord**, Mirela Claudia Rimbu, Cristiana Tanase, *Alkaloid Constituents of Chelidonium majus L.: An Overview of Their Biological Activity and Toxicity,* Conference with international participation of the Faculty of Medicine of Titu Maiorescu University, Transdisciplinary Innovative Approaches in Modern Medicine, VIII edition, Bucharest, May 16-18, 2025
8. Mirela Claudia Rîmbu, **Daniel Cord**, Raluca Neacșa, Cristiana Tănase, Mariana Popescu, *Chemopreventive potential of Taraxacum officinale: a natural approach to cancer prevention* (Abstract), International Conference, Education and creativity for a knowledge based society (18th edition), Universitatea Titu Maiorescu, november 21 - 23, 2024, București

9. Mariana Panţuroiu, Mona Luciana Galățanu, Luiza Mădălina Cima, Roxana Măriuca Gavriloaia, Roxana Colette Sandulovici, Mariana Popescu, **Daniel Cord**, Mirela Claudia Rîmbu, *Evaluation of antioxidant activity and bioactive compound content in Silybum marianum, Cynara scolymus and Taraxacum officinale: Synergistic potential and therapeutic implications*, International Conference, Education and creativity for a knowledge based society (18th edition), Universitatea Titu Maiorescu, november 21 - 23, 2024, București

10. Mirela Mihăilă, Marinela Bostan, Viviana Roman, Camelia Hotnog, Mariana Popescu, Roxana Colette Sandulovici, **Daniel Cord**, Mirela Claudia Rimbu, *Compositional study and evaluation of the antiproliferative action of Chelidonium majus extract on tumor cell lines*, The 10th Congress of the Federation of the Romanian Cancer Society, the 30th Congress of the Romanian Society of Radiotherapy and the 35th Congress of the Romanian Society of Radiotherapy and Medical Oncology, 24-27.10.2024, Sinaia, Romania (poster)